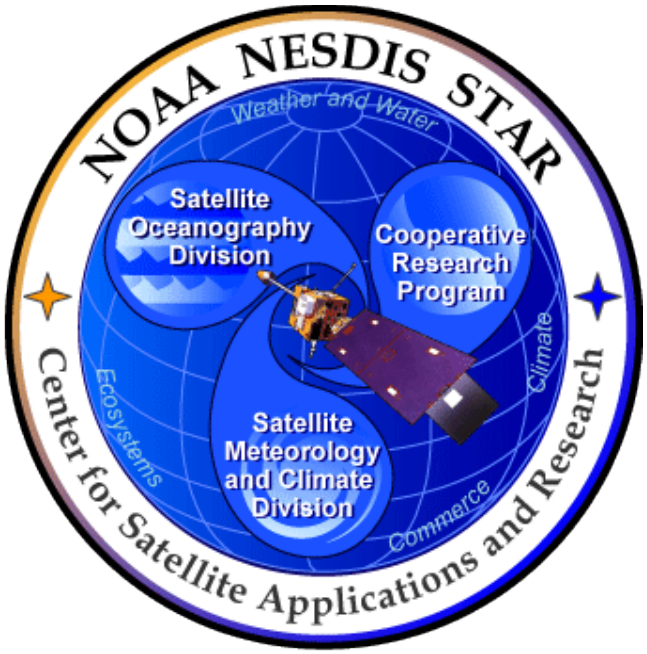

NOAA NESDIS
CENTER for SATELLITE APPLICATIONS and RESEARCH

ALGORITHM THEORETICAL BASIS DOCUMENT

A Naïve Bayesian Cloud Mask Delivered to NOAA Enterprise

Andrew Heidinger, NOAA/NESDIS/STAR
Denis Botambekov, CIMSS
Andi Walther, CIMSS

Version 1.1

October 14, 2016

TABLE OF CONTENTS

LIST OF FIGURES

LIST OF TABLES

LIST OF ACRONYMS

1DVAR - one-dimensional variational
ABI - Advanced Baseline Imager
AIT - Algorithm Integration Team
ATBD - algorithm theoretical basis document
A-Train – Afternoon Train (Aqua, CALIPSO, CloudSat, etc.)
APOLLO – AVHRR Processing Scheme over Land, Clouds and Ocean
AVHRR - Advanced Very High Resolution Radiometer
AWG - Algorithm Working Group
CALIPSO - Cloud-Aerosol Lidar and Infrared Pathfinder Satellite
CASPR – Cloud and Surface Parameter Retrieval
CIMSS - Cooperative Institute for Meteorological Satellite Studies
CLAVR-x - Clouds from AVHRR Extended
CLAVR-1 Clouds from AVHRR Phase 1
CRTM - Community Radiative Transfer Model (CRTM)
ECM – NOAA Enterprise Cloud Mask
ECWMF - European Centre for Medium-Range Weather Forecasts
EOS - Earth Observing System
EUMETSAT- European Organization for the Exploitation of Meteorological Satellites
F&PS - Function and Performance Specification
GFS - Global Forecast System
GOES - Geostationary Operational Environmental Satellite
GOES-RRR – GOES-R Risk Reduction
IR – Infrared
IRW – IR Window
ISCCP – International Satellite Cloud Climatology Project
MODIS - Moderate Resolution Imaging Spectroradiometer
MSG - Meteosat Second Generation
NASA - National Aeronautics and Space Administration
NCEP – National Centers for Environmental Prediction
NESDIS - National Environmental Satellite, Data, and Information
NOAA - National Oceanic and Atmospheric Administration
NWP - Numerical Weather Prediction
PFAAST - Pressure layer Fast Algorithm for Atmospheric Transmittances
PLOD - Pressure Layer Optical Depth
POES - Polar Orbiting Environmental Satellite
RTM - radiative transfer model
SEVIRI - Spinning Enhanced Visible and Infrared Imager
SSEC – Space science and Engineering Center
SSM/I -- Special Sensor Microwave Imagers
STAR - Center for Satellite Applications and Research
UW – University of Wisconsin-Madison

ABSTRACT

This document describes the algorithm an Enterprise Cloud Mask (ECM), which was delivered to the NOAA Enterprise. The ECM utilizes the Naïve Bayesian idea of clear/cloudy pixels detection. The retrieved properties of the ECM are a 4-level cloud mask (clear, probably clear, probably cloudy, cloudy), and cloud probability (0.0 - 1.0).

The 11-micron channel has always been a primary source of cloud discrimination in all-current geostationary and polar sensors. However, the ECM uses a wide variety of bands, which vary from sensor to sensor. It allows for information from the reflective, water vapor and infrared bands to be used in cloud discrimination. The ECM incorporates tests and advancements from other cloud detection groups, including a test that restores clouds in the terminator region, where cloud detection has limited performance. The ECM can run on VIIRS, MODIS, AVHRR, GOES, SEVIRI, AHI, COMS, etc.

The document first describes the satellite, ancillary and derived data used in the ECM. Then it describes the physical basis and the various tests used in the ECM as well as how the clear sky reflectance is calculated. Finally, the results from the VIIRS validated against the MODIS cloud mask algorithm, the official EUMETSAT cloud mask algorithm as well as the CALIOP lidar.

1 INTRODUCTION

1.1 Purpose of this Document

The primary purpose of this ATBD is to establish guidelines for producing the 4-level cloud mask and cloud probability from sensors flown on geostationary and polar meteorological satellites. This document will describe the required inputs, the theoretical foundation of the algorithms, the sources and magnitudes of the errors involved, practical considerations for implementation, and the assumptions and limitations associated with the product, as well as provide a high level description of the physical basis for the initial estimate of the presence or absence of cloud within each pixel. The cloud mask is made available to all subsequent algorithms that require knowledge of the presence of cloud.

1.2 Who Should Use this Document

The intended users of this document are those interested in understanding the physical basis of the algorithms and how to use the output of this algorithm to optimize the cloud detection for their particular application. This document also provides information useful to anyone maintaining or modifying the original algorithm.

1.3 Inside Each Section

This document is broken down into the following main sections.

- **System Overview**: provides a brief description of the products generated by the algorithm.
- **Algorithm Description**: provides a detailed description of the algorithm including its physical basis, its input and its output.
- **Assumptions and Limitations**: provides an overview of the current limitations of the approach and notes plans for overcoming these limitations with further algorithm development.

1.4 Related Documents

This document currently does not relate to any other document and to the references given throughout.

1.5 Revision History

Version 1.0 of this document was created by Dr. Andrew Heidinger of NOAA/NESDIS, Denis Botambekov of CIMSS/SSEC/UW-Madison and its intent was to accompany the delivery of the version 1.0 algorithm to the AIT NOAA Enterprise Team. In Version 1.1 several minor changes made to reflect spring 2016 ECM code delivery to AIT.

2 OBSERVING SYSTEM OVERVIEW

This section describes the products generated by the NOAA Enterprise Cloud Mask (ECM) and its associated sensor requirements.

Table 1. JPSS Clear sky Mask Product Requirements (L1RDS-2457)

Attribute	Threshold	Objective
Cloud Mask Applicable Conditions: 1. Requirements apply whenever detectable clouds are present. 2. Cloud Mask shall be computed and reported for the total cloud cover		
a. Horizontal Cell Size	0.8 km at Nadir	NS
b. Cloud Mask Horizontal Reporting Interval	Cloud Mask HCS	NS
c. Mapping Uncertainty, 3 Sigma	4 km	1 km
d. Cloud Mask Measurement Range	Cloudy/Not Cloudy	NS
e. Cloud Mask Probability of Correct Typing		
1. Ocean, Day, COT > 1.0 (2)	94%	NS
2. Land, Day, COT > 1.0	90%	NS
3. Ocean, Night, COT > 1.0	85%	NS
4. Land, Night, COT > 1.0	88%	NS
f. Cloud Leakage Rate		
1. Ocean, Day, COT > 1.0, outside Sun Glint region (2)	1%	NS
2. Land, Day, COT > 1.0	3%	NS
3. Land, Ocean, Night, COT > 1.0	5%	NS
g. False Alarm Rate		
1. Ocean, Day, COT > 1.0 (2)	5%	NS
2. Land, Day, ToC NDVI <0.2 or ToC NDVI > 0.4, or Desert, COT > 1.0	7%	NS
3. Land, Ocean, Night, COT > 1.0	8%	NS
h. Refresh	At least 90% coverage of the globe every 12 hours (monthly average)	4 hrs.
		v2.5, 1/23/13

Notes:
1. Attribute (a) shows the Cloud Map HCS as 0.8 km which is approximately the VIIRS M band Nadir pixel size.
2. Cloud Optical Thickness (COT) is different as the extinction (scattering plus absorption) per unit length, integrated over each and every distinguishable cloud layer in a vertical column and all distinguishable cloud layers in aggregate, in a vertical column of the atmosphere.

2.1 Products Generated

The cloud mask algorithm is responsible for the initial cloud detection field for all imager pixels. In terms of the JPSS Program Level 1 Requirements Document (L1RD) and L1RD SUPPLEMENT (L1RDS), it is responsible directly for the Clear Sky Mask product within the Radiance Product Category. However, the cloud mask will be used by most of the algorithms that require knowledge of the presence or absence of cloud within a given pixel. The current cloud mask requirement calls for a four-level (Confidently/Probably Clear, Confidently/Probably Cloudy) cloud mask. The ECM also

generates cloud probability (from 0 to 1). In addition, the cloud mask output will include all test results that were used to determine the final four-level mask to allow for modification by downstream users. The requirements for the clear sky mask from the L1RDS version 2.5 are stated below in Table 1.

2.2 **Instrument Characteristics**

The cloud mask will be produced for each pixel observed by the imager sensor. The final channel set depends on sensor characteristics (band availability). Table 2 summarizes the wavelengths if available would be used by the ECM. Note, the ECM is designed to work even when only a subset of the expected channels is provided. For example, when used with VIIRS data, the ECM is able to account for the lack of water vapor channels. The ECM also works with data from the GOES, SEVIRI, AHI, AVHRR, MODIS, etc. imagers.

Table 2. Channel wavelengths used by the ECM.

Wavelength (μm)
0.659
0.865
1.64
2.13
0.415
1.375
3.75
4.05
6.715
8.55
11.03
12.02
0.7 (VIIRS DNB)

The algorithm relies on spectral and spatial tests. The performance of the cloud mask is therefore sensitive to any imagery artifacts or instrument noise. Calibrated observations are also critical because the cloud mask compares the observed values to those from a forward radiative transfer model. We are assuming the performance outlined in this section during our development efforts.

3 ALGORITHM DESCRIPTION

This section provides a complete description of the algorithm at the current level of maturity (which will improve with each revision).

3.1 Algorithm Overview

The cloud mask serves a critical role in the Enterprise processing system. It is a fundamental cloud property in itself but also serves to determine which pixels can be used for clear-sky applications (SST, NDVI, etc.). The following heritage cloud mask algorithms have influenced the ECM:

- The MOD/MYD35 MODIS cloud mask from UW CIMSS
- The Clouds and the Earth's Radiant Energy System (CERES) MODIS cloud mask from NASA Langley Research Center
- CASPR cloud mask used in the AVHRR Polar Pathfinder Extended (APP-x)
- GOES-R Baseline Cloud Mask

As with the above masks, the ECM combines spectral and spatial tests to produce a 4-level classification of cloudiness. The 4-levels of the ECM cloud mask are:

- Clear,
- Probably Clear,
- Probably Cloudy, and
- Cloudy.

These categories are the same as those employed in the CLAVR-x and MYD35 masks. In general, the cloud mask is designed so that the clear and cloudy pixels are suitable for clear and cloudy product generation.

In addition to the 4-levels of cloudiness, the ECM also provides the results of every test used to compute the 4-level mask, and cloud probability (0 – 1). This information is provided to allow other applications to modify the cloud mask to suit their specific needs.

3.2 Processing Outline

The processing outline of the ECM is summarized in Figure 1 below. The current ECM is implemented within the Enterprise system. The Enterprise provides all of the observations and ancillary data, such as the data from the NWP and RTM. The ECM is designed to run on segments of data where a segment is comprised of multiple scan lines.

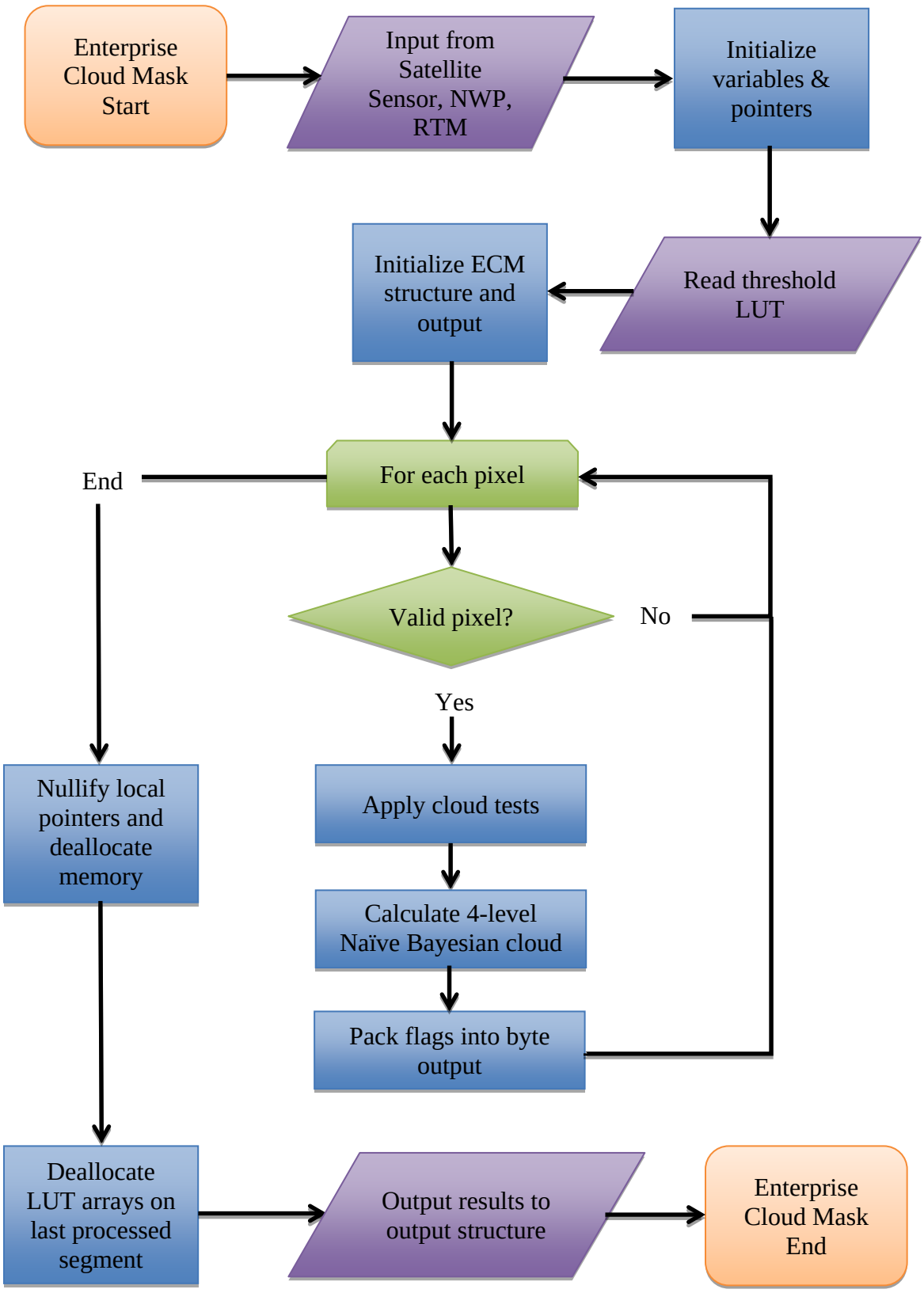

Figure 1. High Level Flowchart of the ECM illustrating the main processing sections.

3.3 Algorithm Input

This section describes the input needed to process the ECM. While the ECM is derived for each pixel, it does require knowledge of the surrounding pixels. Currently, the ECM is run on segments that contain 200 scan-lines. While the final size of the segments is to be determined, the ECM should not be run with information from only one pixel.

3.3.1 Primary Sensor Data

The list below contains the primary sensor data used by the ECM. By primary sensor data, we mean information that is derived solely from the imager sensor observations and geolocation information. The ECM uses the following available channels based on the particular sensor.

- Calibrated solar reflectance percent (0-100%) for 0.415, 0.659, 0.865, 1.24, 1.375, 1.64, 2.13, 3.75 micron channels.
- Calibrated radiances for 3.75 and 11.0 micron channels.
- Calibrated brightness temperatures for all IR channels.
- Calibrated lunar reflectance percent (0-100%) VIIRS Day-Night Band (DNB).
- Bad pixel mask for each channel.
- Space mask.
- Derived 3.75 micron channel emissivity, which is described Section 1.9.3.
- 3.75 micron channel solar energy ($mW/m^2/cm^{-1}$).
- Sensor viewing zenith angle.
  NOTE: For geostationary satellites the requirement is to produce the clear sky mask out to a sensor zenith angle of 70^o.
- Solar zenith angle.
- Relative azimuth angle.
- Glint zenith angle.
- Scattering angle.
- Cosine of sensor, scattering and solar zenith angles.
- Number of lines and elements for the given segment.

3.3.2 Ancillary Data

The following data lists the ancillary data required to run the ECM. By ancillary data, we mean data that requires information not included in the sensor observations or geolocation data. The NWP and RTM data, which are at NWP resolution, are interpolated to pixel level.

- **Numbers of elements, lines, maximum lines, and segments to process**
- **Latitude, Longitude of each pixel**
- **Invalid data mask**

- **Sun earth distance**

- **Surface type**

- **Surface elevation**
  Both the surface height and maximum surface elevation in a 3x3 box are used in the ECM

- **Land mask**
  Using the land mask, each pixel is flagged internally as land or water.

- **Coast mask**
  Using the coast mask, each pixel is flagged internally as coast or not coast.

- **Ocean glint mask**
  Pixels are set to glint or no glint

- **Snow mask**
  Using the snow mask, each pixel is flagged internally as snow or clear. In addition, if a pixel has an 11 μm brightness temperature of greater than 277K, the snow mask is turned off.

- **Surface emissivity of 3.75 micron channel from SEEBOR**

- **NWP level associated with the surface**

- **NWP level associated with the tropopause**

- **Viewing Zenith and Azimuth Angles**

- **Solar Zenith and Azimuth Angles**

- **NWP Line and element indices**

- **Sea Surface Temperature Uniformity**

- **Surface temperature from NWP**

- **Surface temperature uniformity from NWP**

- **Total perceptible water from NWP**

- **Total column ozone from NWP**

- **Clear-sky Infrared RTM Calculations**
  - Clear-sky top-of-atmosphere (TOA) BTs for 3.75 micron channel.
  - Clear-sky TOA brightness temperatures computed for 6.7, 11.0 and 12.0 micron channels.
  - Clear-sky, and 3x3 median emissivity for 3.75 micron channel.
  - Equivalent blackbody radiance of a cloud emitting at the temperature of the tropopause for 11.0 micron channel.

- **Clear-sky Reflectance**
  - The clear sky reflectance is first corrected for atmospheric scattering by adding in the Rayleigh single scattering reflectance and transmission.
  - In the terminator region, the clear sky reflectance is renormalized.
  - The clear sky reflectance for each pixel, the standard deviation, and minimal value of the clear sky 0.65 micron channel reflectance over a 3x3 pixel array are used.
  - Clear-sky TOA reflectance for 1.60 micron channel.
  - Clear-sky TOA reflectance for 3.75 micron channel.

3.3.3 Derived Data

The following lists and briefly describes the data that are required by the ECM that are provided by other algorithms.

- **Valid pixel mask**
  A pixel is determined to be valid if it is not a space pixel, has a sensor zenith angle of less than 70^{o}, and has a valid measured and clear sky 11μm brightness temperature.

- **Correlation of channel 6.7 μm brightness temperature to channel 11.0 μm brightness temperature**
  The ECM computes the Pearson Correlation Coefficient between the 6.7 and 11.0 μm channel brightness temperatures for each pixel.

- **Derived 11.0 μm channel top of the tropopause emissivity**
  The ECM derives the 11.0 micron channel top of troposphere emissivity using the measured radiance, clear sky radiance, space mask, latitude/longitude cell index from the NWP, tropopause index from the NWP, viewing zenith angle bin index, and 11.0 micron channel blackbody radiance. Both the 11.0 μm top of troposphere emissivity for each pixel and the LRC top of troposphere emissivity for each pixel are required.

- **Minimum 0.65 μm channel reflectance over a 3x3 pixel array**

- **Standard deviation 0.65 μm channel reflectance over a 3x3 pixel array**

- **Maximum 11.0 μm brightness temperature over a 3x3 array**

- **Standard deviation of the 11.0 μm channel brightness temperature over a 3x3 pixel array**

- **Glint mask**
  A glint mask is initially defined based upon the glint zenith angle. Any non-land and snow-free pixels that have a glint zenith of less than 40^o are classified as "glint." However, those pixels that have been marked as glint and have an 11μm brightness temperature of less than freezing (273.15K), or the 11μm brightness temperature is less than the clear sky 11μm brightness temperature minus 5.0, have the glint flag turned off. Turning the glint mask off is an attempt to restore cold pixels in the glint zone. Further checks are to look at pixels that have a uniform performance. A check is done by checking to see if a glint pixel has a standard deviation of 0.64μm reflectance over a 3x3 pixel array greater than 1.0. If it does, the pixel is restored to non-glint.

3.3.3.1 Rayleigh Scattering

The Rayleigh or molecular scattering optical is taken from the cloud mask threshold include file and is not computed during execution. For EBI, we have estimated that the total in-band to 0.63 μm channel Rayleigh optical depth is approximately 0.05. The Rayleigh phase function is used to account for the angular distribution of the Rayleigh scattering.

$$P_{Ray} = 0.75(1+\mu^2) \qquad (1)$$

where μ is the cosine of the scattering angle where scattering angle is defined by the solar and viewing geometries.

3.3.3.2 Aerosol Scattering

To model the aerosol scattering, a Henyey-Greenstein phase function was assumed as illustrated below.

$$P_{aer} = (1-g_{aer}{}^2) \Big/ (1+g_{aer}{}^2 - 2g_{aer}\mu)^{3/2} \qquad (2)$$

In the above equation, g_{aer} is the asymmetry parameter. The single scatter albedo ($\omega_{o,aer}$), g_{aer} and total column aerosol optical depth, τ_{aer}, are provided in the cloud mask threshold include files.

3.3.3.3 Gaseous Absorption

The main absorbing gases in 0.63 μm channel are water vapor and ozone. The total column optical depths (*t*) are computed using polynomial regressions based on the total precipitable water (*TPW*) and total column ozone (*TOZONE*).

$$\tau_{h_2o} = a + b(TPW) + c(TPW^2) \quad (3)$$

$$\tau_{o_3} = a + b(TOZONE) + c(TOZONE^2) \quad (4)$$

The coefficients (*a, b, c*) for the water vapor and ozone optical depth regressions were computed using MODTRAN4 and the assumed 0.63 µm channel spectral response functions. For use in this routine, the ozone and water vapor optical depths are combined in one gaseous optical depth, τ_{gas}.

$$\tau_{gas} = \tau_{h_2o} + \tau_{o_3} \quad (5)$$

3.3.3.4 Computation of Clear-sky Reflectance

The computation of the clear-sky 0.63 µm channel reflectance is done by combining a single scattering approximation coupled with an isotropic two-stream approximation. This formulation is a modified version of that used by the MODIS Atmospheres Science Team and described by Wang and King (1997).

To compute the clear-sky reflectance, several intermediate terms are needed. First, a total optical depth, τ_{total}, is computed from the Rayleigh, aerosol and gas optical depths.

$$\tau_{total} = \tau_{Ray} + \tau_{aer} + \tau_{gas} \quad (6)$$

In addition, a total optical depth for isotropic scattering computed as follows

$$\tau_{iso,total} = \tau_{Ray} + (1 - g_{aer})\tau_{aer} + \tau_{gas} \quad (7)$$

where the aerosol optical depth is scaled by $1 - g_{aer}$. The effective single scatter albedo, ϖ_o, of the entire column is computed as

$$\varpi_o = (\varpi_{o,aer}\tau_{aer} + \tau_{ray}) \Big/ \tau_{total} \quad (8)$$

and the effective phase function, *P*, of the entire column is computed as

$$P = (\varpi_{o,aer}\tau_{aer}P_{aer} + \tau_{Ray}P_{Ray}) \Big/ \tau_{scat,total} \quad (9)$$

where $\tau_{scat,total}$ is the total scattering optical depth.

$$\tau_{scat,total} = \tau_{Ray} + \omega_{o,aer}\tau_{aer} \quad (10)$$

The 0.63 µm channel clear-sky reflectance, $R_{2,clear}$ is computed from three terms. The first term, R_a, accounts for the single scattering contribution of the atmosphere. R_a is computed using the following relation

$$R_a = \left(\varpi_o P \Big/ (4m\mu_v\mu_o) \right)(1 - \mathrm{T}_{ss}) \tag{11}$$

where m is the airmass factor ($1/\mu_v + 1/\mu_o$) $_{ss}$ is the single-scattering transmission term computed as

$$\mathrm{T}_{ss} = e^{-(\tau_{total}/\mu)} \tag{12}$$

The second term, R_b, accounts for the contribution of reflectance scattered in the atmosphere and then scattered off the surface and is computed as follows

$$R_b = \tau_{iso,scat,total} \Big/ (2\mu_o)\, \mathrm{T}_{iso,total,view}\, \alpha_{sfc} \tag{13}$$

where α_{sfc} is the surface albedo, and $T_{iso,total,view}$ is the transmission term computed along the viewing direction assuming isotropic scattering.

$$\mathrm{T}_{iso,total,view} = e^{-(\tau_{iso,total}/\mu)} \tag{14}$$

The third term, R_c, is the contribution of reflectance scattered off the surface from the direct solar beam and then scattered in the atmosphere. This term is given by

$$R_c = \tau_{iso,scat,total} \Big/ (2\mu_v)\, \mathrm{T}_{iso,total,sun}\, \alpha_{sfc} \tag{15}$$

where

$$\mathrm{T}_{iso,total,sun} = e^{-(\tau_{iso,total}/\mu_o)} \tag{16}$$

The final clear-sky 0.63 µm channel reflectance is computed simply as

$$R_{2,clear} = 100(R_a + R_b + R_c) \tag{17}$$

where the factor converts the reflectance to a percentage.

3.4 Theoretical Description

Cloud detection is the process of separating cloudy from clear pixels. It always involves assumptions of the radiometric characteristics of the clear and/or cloudy state and looking for departures from them. In the ECM, spectral, and spatial tests are used to look for clouds by identifying pixels that do not exhibit the expected behavior of the clear-sky

state. Each test described is applied to each pixel, resulting in a cloud/no cloud score, which is then used to decide whether a pixel is cloudy or clear.

3.4.1 Physics of the Problem

The challenge for any cloud mask is to exploit spectral, spatial and temporal signatures that maximize the sensitivity to the presence of cloud while simultaneously minimizing the false detection of cloud. The ECM algorithm makes extensive use of information from NWP fields, coupled with a Radiative Transfer Model (RTM), to generate the expected clear-sky state for the spectral tests. This approach has also been adopted by EUMETSAT (Dybrroe et al., 2005). While the current NWP fields often have errors in some critical fields, such as the surface temperature over land, they provide needed and useful information. Over the coming years before the launch of GOES-R, the NWP fields are expected to improve in both accuracy and spatial resolution. For the spatial thresholds, we have no reliable information from the NWP fields and must rely on other sources. For example, the thresholds for the spatial uniformity tests rely on information from pre-computed high resolution maps of surface elevation and surface reflectance (see Section 1.9.2).

In addition, the spectral tests are broken into those that use infrared channels, shortwave infrared, and solar-reflectance channels. All applicable tests are used to construct the ECM using Naïve Bayesian approach. However, users that wish to have a cloud mask with consistent day-night performance are encouraged to use the cloud mask generated *without* the solar reflectance tests considered.

The other major type of test in the ECM is the restoral test. The restoral tests are separated into tests that "restore" probably cloudy pixels to clear pixels and tests that "restore" cloudy pixels to probably cloudy pixels. As defined, the effect of these restoral corrections is to provide a conservative estimate on cloudiness (i.e., minimize false alarms in the ECM). Note many of the cloud detection names arise from the Clouds from AVHRR (CLAVR) cloud mask developed by Stowe et al. (1999).

3.4.1.1 Use of CALIPSO Data in Determining Cloud Mask Classifiers

An important part in the development of ECM is the use of CALIPSO observations to help define the classifiers. Because CALIPSO provides one of the most unambiguous and direct measures of the presence of the highest cloud layers (i.e., those also observed by the passive sensors), it has been used to help understand the behavior of each cloud mask test for clear and cloudy pixels. While many cloud masks have used RTM simulations to set cloud detection thresholds (i.e., CASPR), the goal of the ECM is to use the availability of pixel-level clear-sky information to derive new cloud mask metrics that maximize the separation of cloudy and clear pixels. The main advantage of using an observationally based approach (collocation of CALIPSO and passive sensor test data) to threshold definition is that simulations may not capture the true variability present in real scenes. The ECM allows for threshold modification when warranted.

In this analysis, the 1 km cloud layer product from the standard CALIPSO processing (Vaughan et al., 2005) was used together with data from the MODIS Aqua and VIIRS SNPP instruments. A key component of this analysis is the ability to co-locate the passive sensor with CALIPSO. To accomplish this, a routine was developed to find the passive sensor pixel that was closest in distance to each 1km CALIPSO cloud-layer pixel. This routine employed a nearest neighbor approach coupled with a polynomial fit to provide initial estimates of collocated pixels. The CALIPSO product, developed by NASA Langley, provides top, base and number of cloud layers for up to 10 layers in a 1 km footprint, and attempts to distinguish cloud from aerosol, smoke and dust. For the purposes of this study, a cloud mask from CALIPSO was determined noting the number of cloud layers in each 1 km pixel (column). Any CALIPSO column with more than zero cloud layers was assigned to the cloudy category. In addition, a cloud fraction from CALIPSO was computed using results from all lidar fields of view that fell within each MODIS/VIIRS pixel. Using the method described in Heidinger and Pavolonis (2009), the temperature of the highest cloud layer is used in conjunction with the 11 μm clear radiance calculation and 11 μm MODIS/VIIRS observations to compute an 11 μm cloud emissivity. This value represents the emissivity that a cloud must have if it existed at the level measured by CALIPSO with the observations measured by the passive sensor (i.e., SEVIRI, VIIRS, MODIS, etc.). This is hereafter referred to as the CALIPSO emissivity.

As a lidar with an inherent vertical resolution of 30 m, CALIPSO can detect clouds with opacities and spatial scales far exceeding the capabilities of passive visible/infrared sensors such as MODIS or the VIIRS. In order to use CALIPSO to determine meaningful thresholds for passive detection of clear and cloudy conditions, filtering is required to attempt to make the CALIPSO detection comparable to the performance expected from the passive observing system. In this analysis, we ignored all CALIPSO results which had cloud fractions between 0.1 and 0.9. The purpose of this filter is to restrict the analysis to CALIPSO data that is uniform over the spatial scales of the coarser MODIS or VIIRS pixels. In addition, a threshold of 0.1 was applied to the CALIPSO emissivity in an attempt to remove from consideration any pixels with very low optical depths that would fall below the detection capabilities of the channels on the passive sensors.

In the remaining part of this section, CALIPSO data matched in space and time with MODIS or VIIRS observations are used to demonstrate the skill of the cloud mask tests in the ECM.

3.4.1.2 Naïve Bayesian Formulation

In the full or classical Bayesian approach, the probability of a given passive satellite pixel being cloudy for a set of features (F) is given by $P(C_{yes}|F)$ defined as

$$P(C_{yes}|F) = \frac{P(C_{yes})P(F|C_{yes})}{P(F)} \qquad (18)$$

where $P(C_{yes})$ is the prior probability of any pixel being cloudy without any knowledge of F and $P(F)$ is the probability of existence of the pixel's set of features (F). $P(F|C_{yes})$ is the probability of the existence of the pixel's set of features for the cloudy pixels. The components in the feature set F are referred to as the cloud mask classifiers and the particular features employed in this approach are described in Section 1.10.1.4. The Bayesian context, $P(F|C_{yes})$ is referred to as the posterior probability.

One issue with the classical Bayesian approach is the use of N classifiers requires the computation of NxN dimensioned arrays holding the class conditional probabilities. In most cloud detection approaches, several tests are required to fully detect all types of cloudiness in visible/infrared imagery. To put this in perspective, while the CALIPSO-AVHRR collocation process described above resulted in over 5 million pixels for the twelve month period studied, that number is not sufficient to fully populate the NxN space required for the cloud mask classifiers used in this algorithm especially given the need to compute these classifier distributions for several surface types. To overcome this we have employed a naïve Bayesian approach. In the Naïve Bayesian assumption, each of the feature probabilities can be treated as independent, and the value of $P(C_{yes}|F)$ can be rewritten as follows:

$$P(C_{yes} \mid F) = \frac{P(C_{yes}) \prod_{i=1}^{N} P(F_i \mid C_{yes})}{P(F)} \qquad (19)$$

The denominator in the above equation, $P(F)$, is computed as

$$P(F) = P(C_{yes}) \prod_{i=1}^{N} P(F_i \mid C_{yes}) + P(C_{no}) \prod_{i=1}^{N} P(F_i \mid C_{no}) \qquad (20)$$

where $P(C_{no})$ is the prior probability of any pixel being clear $(P(C_{no}) = 1 - P(C_{yes})$.

The obvious advantage of this method is the use of N classifiers (or cloud mask tests) requires generation of N, not NxN, dimensioned arrays. While this approximation may seem severe, Naïve Bayesian approaches have been applied successfully to many complex detection problems (Kossin and Sitkowski, 2009).

To generate the clear and cloudy classifier distributions, three filters were applied to the data. First, memory limitations required a thinning of the data by a factor of two. Second, only co-locations that occurred with a time difference of less than 10 minutes were used. To avoid the increased uncertainty in the co-location process for sub-pixel cloudiness, only pixels where the CALIPSO cloud fraction was either 0 or 1.0 were included. Next, the classifiers were computed separately for different regions or surface types. The selection of these surface types is discussed below. Figure 2 shows an example set of clear and cloudy classifier distributions computed for one classifier (T_{max}-T) over the DEEP OCEAN surface type. The T_{max}-T classifier is described in the next section. The clear and cloudy distributions are normalized to unity for clarity of presentation. Also shown in Figure 2 is the posterior probability as a function of the classifier. For

illustrative purposes Figure 2 assumes only the use of one classifier while in the full approach all classifiers are used in Eq. 20. Figure 2 does illustrate one of the key strengths of the Bayesian approach in that the probability of cloud varies smoothly over the range of the classifier. In threshold-based techniques, the probability distributions are assumed to jump from 0 to 1 when passing over the chosen threshold.

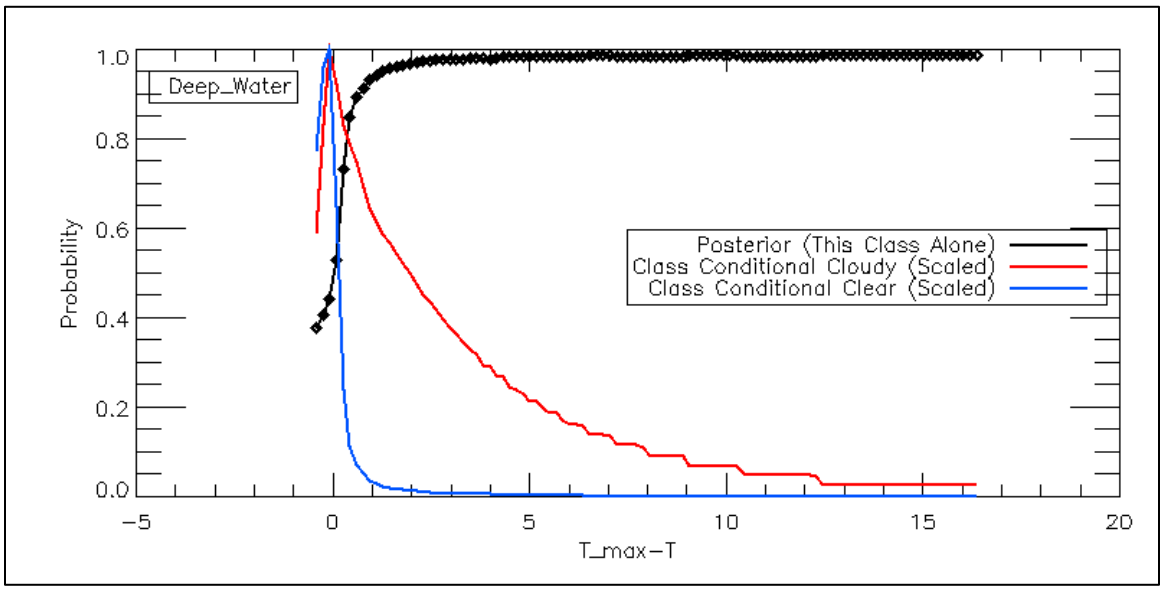

Figure 2. Conditional classifier distributions for the T_{max}-T metric for the Deep-Ocean classifier.

(T_{max}-T is the difference between the warmest 11 μm brightness temperature over a 5x5 array centered on a pixel and the pixel's 11 micron brightness temperature. The red line shows the conditional classifier for clear results and the blue line shows the conditional classifier for cloudy results. The black line shows the posterior probability computed using this classifier alone. The cloudy and clear classifiers are normalized to unity for clarity.)

3.4.1.3 Selection of Surface Types

As stated above, the selection of different surface types to generate the classifiers is critical. We have chosen to classify the globe into seven surface types. The goal of classifying different surface types is to capture the systematic biases in our knowledge of the clear-sky conditions that vary greatly from one surface type to another. In the current algorithm, we classify the globe into the following surface types: 1-DEEP OCEAN, 2-SHALLOW WATER, 3-LAND, 4-SNOW, 5-ARCTIC, 6-ANTARCTIC, and 7-DESERT. These surface types were chosen after a series of trial and error experiments. Each surface type represents a region where the distribution in the contrast between clear and cloudy skies and the accuracy of the performance of the clear-sky model is similar. The inputs to the surface type are the land cover data from the land cover data base used in the MODIS geolocation file (MOD/MYD03), the snow field within the NCEP reanalysis (Kalnay et al, 1996), the NOAA Optimum Interpolation Sea Surface

Temperature Version 2 (OISST) daily 25 km SST analysis (Reynolds et al., 2002) and 3.75 μm surface emissivity from the SEEBOR surface emissivity data base (Seeman et al, 2008). Figure 3 shows the global distribution of these surface types for January 1 and July 1, 2009. A brief description of these types follows. The surface types will vary with the frequency of the ancillary data. While the land cover data is temporally invariant, the surface emissivity values vary every 16 days. The largest driver of the surface type variation is the snow and ice cover information.

The sea-ice information is taken from the OISST data and varies daily. The snow information is taken from the NCEP Reanalysis, which is updated every 6 hours.

DEEP OCEAN
The DEEP OCEAN surface type consists of pixels where the MOD03 land mask was set to "Deep Ocean" and the sea-ice information from the OISST data indicated ice-free conditions. Highly accurate clear-sky radiative transfer modeling and spatially uniform surfaces characterize the DEEP OCEAN surface type.

SHALLOW WATER
The SHALLOW WATER surface type is defined by ice-free pixels that the MOD03 land mask classified as Moderate Ocean, Deep-Inland-Water and Shallow-Inland Water. In addition, any pixels where the 3x3 standard deviation of the background SST from the OISST exceed 1.0 K were also included in the SHALLOW WATER surface type. In general, this surface type includes water bodies where our knowledge of the surface temperature is much less accurate than that of the DEEP OCEAN surface type.

LAND
The LAND surface type includes all land surfaces that are not covered by snow and not classified as desert.

SNOW
The SNOW surface type includes all land surfaces covered by snow excluding Antarctica and Greenland.

ARCTIC
The ARCTIC surface type includes all pixels labeled as sea-ice in the Northern Hemisphere.

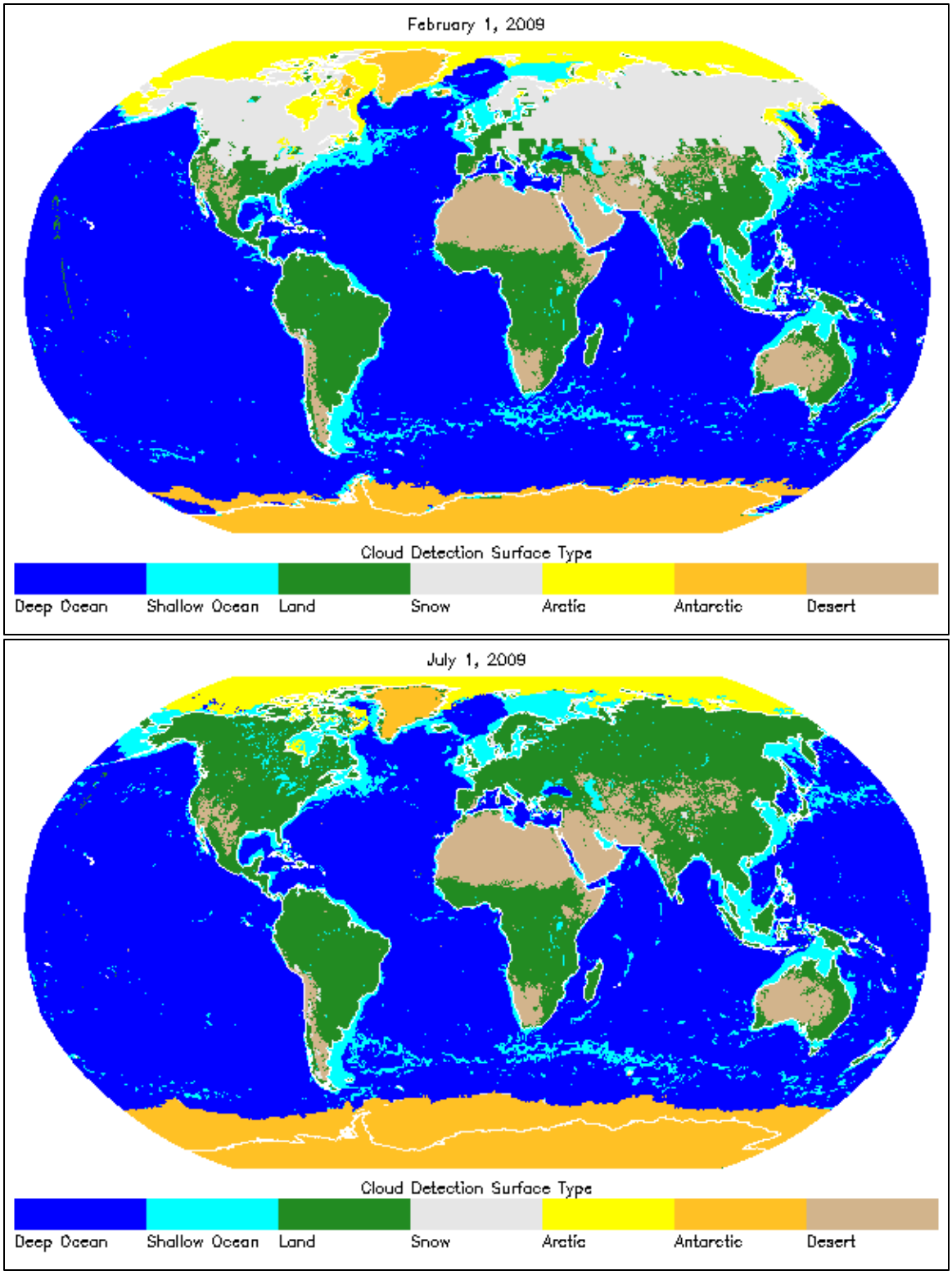

Figure 3. Surface types used to define the Bayesian Classifiers

ANTARCTICA
The ANTARCTICA surface type includes all sea-ice in the Southern Hemisphere and all snow covered surfaces south of 60S. Based on guidance from the MODIS cloud mask team located at the University of Wisconsin, Greenland was also included in the ANTARCTICA surface type.

DESERT
The DESERT surface type includes all pixels with a 3.75 μm surface emissivity less than 0.90 that occurred within 60 latitudinal degrees of the equator. The use of the 3.75 μm emissivity was used to ensure optimal performance for the 3.75 μm classifiers.

Figure 3 shows the global distribution of the surface types for February 1, 2009 (top) and July 1, 2009 (bottom). As Figure 3 shows, the spatial coverage of these surface types varies with season with snow-covered land showing the most dramatic variation. The appearance of SHALLOW OCEAN away from the coasts is due to the inclusion of heterogeneous SST regions (i.e. oceanic fronts) into this surface type.

3.4.1.4 Cloud Mask Classifiers

The Naïve Bayesian formulation allows for multiple cloud classifiers to be used without the need for large arrays. This section briefly describes each classifier used in the ECM. The same classifiers are used in GOES-R Algorithm Working Group (AWG) cloud mask algorithm. It is important to note that even with limited spectral information, for example by the AVHRR, the number of cloud mask classifiers or tests can be large (≈10). For different sensors a different set of classifiers is used. In the AWG cloud masks, we have decided to prioritize the infrared information to help ensure day/night consistency. In addition, we rely on radiative transfer calculations to reduce artificial sensitivities to variability in viewing geometry and the atmospheric and/or surface state.

3.4.1.4.1 Emissivity Referenced to the Tropopause (ETROP)

The ETROP test assumes that clouds produce colder 11 μm brightness temperatures than what would have been observed under clear-sky conditions. This is limited to 11 micron brightness temperatures between 170K and 310K as well as clear sky 11 micron brightness temperatures of above 24K. Traditionally, infrared window (IRW) brightness temperatures are used in gross contrast tests to identify cold pixels. The ETROP, however, operates on the 11μm emissivity computed assuming the cloud top resides at the Tropopause. This Tropopause-relative emissivity is computed as follows:

$$\varepsilon = (I - I\_clear) / (I\_bb - I\_clear) \qquad (21)$$

where I is the observed radiance**,** I_clear is the computed clear-sky radiance (from the RTM) and I_bb is the equivalent blackbody radiance of a cloud emitting at the temperature of the Tropopause. As noted in the ancillary data section, I_bb is provided to the ECM as an input.

The benefits of the ETROP are that ε has a more direct physical meaning than one based on a brightness temperature. By including the clear-sky radiative transfer through the

computation of ε, the ETROP test should be independent of surface temperature and atmospheric profiles. Because ε is referenced to the Tropopause (recalling again that the cloud top temperature here is assumed to be that of the Tropopause), opaque clouds that are positioned at lower and warmer levels will generate ε values less than one. The Tropopause-relative emissivity approximates the true emissivity only for clouds in the upper Tropopause. In clear conditions, the Tropopause-relative emissivity should approach zero. Negative values are possible when the computed clear-sky radiance is greater than the observed clear sky radiance.

The variation of ε with the true cloud emissivity is shown in Figure 4. The cloud is simulated using an ice cloud located between 300 and 400 hPa in a standard Mid-latitude summer atmospheric profile. The slope is constant and the ratio between the true and the Tropopause emissivity is simply the ε. For clouds within the Troposphere, *I* is always less then *I_bb*, values of ε are less than the actual emissivity.

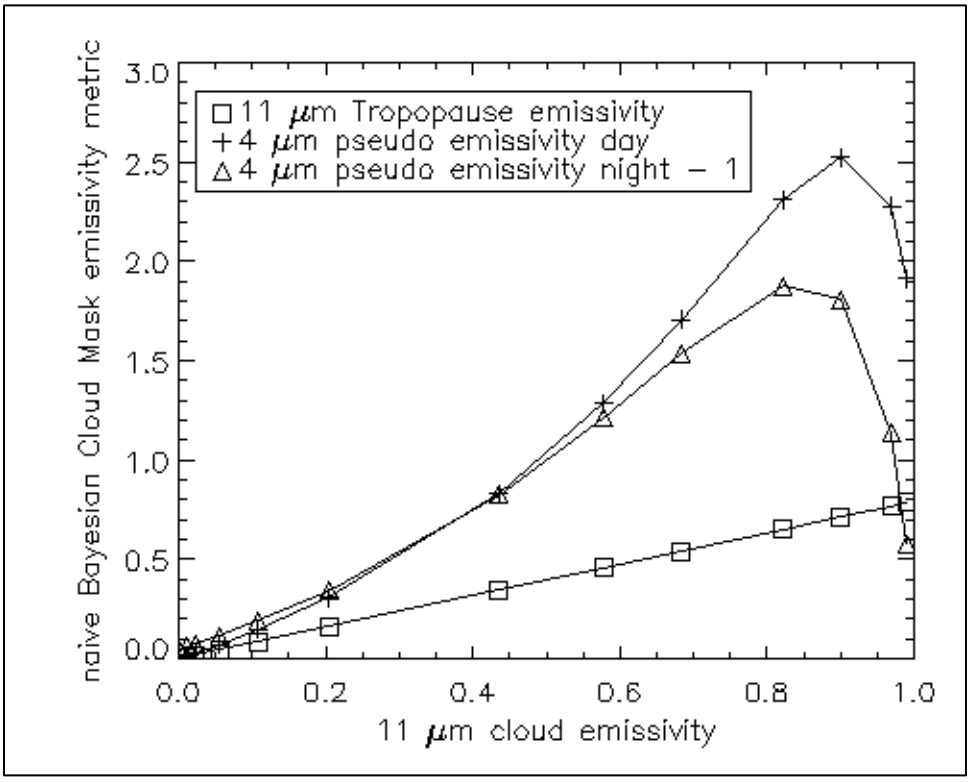

Figure 4. Simulated variation of the emissivity metrics as a function of the true cloud 11 micron emissivity.

(The computations were done for an ice cloud positioned between 300 and 400 hPa in the standard Mid-latitude Summer profile. The daytime results assumed a solar zenith angle of 30^o. The lower surface was ocean. The values plotted are the metrics used in the Naïve Bayesian mask. For clarity, the value of 1 is subtracted from the nighttime 4-micron pseudo emissivity values.)

For the simulation in Figure 4 where the cloud was placed roughly 200 hPa below the Tropopause, the values of ε are roughly 20% less than the true emissivity. Even though the values of ε are much lower for low-level clouds, the accuracy of the clear-sky radiative transfer (especially over oceans) makes the ETROP classifier robust and effective. In clear conditions, the Tropopause emissivity should approach zero. Negative values are possible when the computed clear-sky radiances are greater than the observed clear sky radiances.

3.4.1.4.2 11 μm Thermal Test (BT11)

BT11 is a test which uses brightness temperature (BT) of 11 micron channel. It is a simple test, which is based on the assumption that clouds are in general colder than surface. It compares pixel 11 μm BT to classifier thresholds to determine if the pixel is cloudy or not. This test is good for detecting thick high clouds. The weakness of this test is that it is not always a case. Clouds can be warmer than surface in case of inversion, snow on the ground, etc.

3.4.1.4.3 Relative Thermal Contrast Test (RTCT)

This is a classical Relative Thermal Contrast Test. It is using the difference between maximum 11 μm brightness temperature of a 3x3 box and 11 μm BT (T_{max}-T). This test is very useful for detecting cloud ages. Mountain and coast pixels are excluded from this test.

3.4.1.4.4 11 μm Thermal Uniformity Test (BT11STD)

This test is a variation of Relative Thermal Contrast Test used in the ABI Cloud Mask, but instead of the local 11 μm observations difference (T_{max}-T), BT11STD is based on the standard deviation (STD) of the observed 11 μm brightness temperature computed on a 3x3 box surrounding each pixel. Because of the fact that coasts and mountains are inherently non-uniform, no coast or mountain pixels are used in this test.

Figure 5 shows the variation of the 3x3 11 micron BT STD as a function of CALIPSO cloud fraction.

3.4.1.4.5 11 and 12 μm Split-Window Test (BTD11_12)

Cloud detection tests that use split-window (11 and 12 μm) observations are common in many cloud mask algorithms. For example, they are employed in the MYD35, CASPR, APOLLO and CLAVR-1 schemes. Due to the spectral variation in cloud transmission, the presence of semi-transparent cloud leads to a positive value of the 11-12 μm brightness temperature difference (11-12 BTD). Unfortunately, the physics of water vapor continuum absorption also generate positive values for clear-sky conditions especially for warm and moist atmospheres. More detailed discussions of the use of this information for cirrus cloud detection are given by Inoue (1985) and Prabhakara et al. (1988).

$$\chi = \left(BT_{11} - BT_{12}\right) - \left(BT_{11}^{clear} - BT_{12}^{clear}\right) * \left(BT_{11} - 260.0\right) \Big/ \left(BT_{11}^{clear} - 260.0\right) \qquad (22)$$

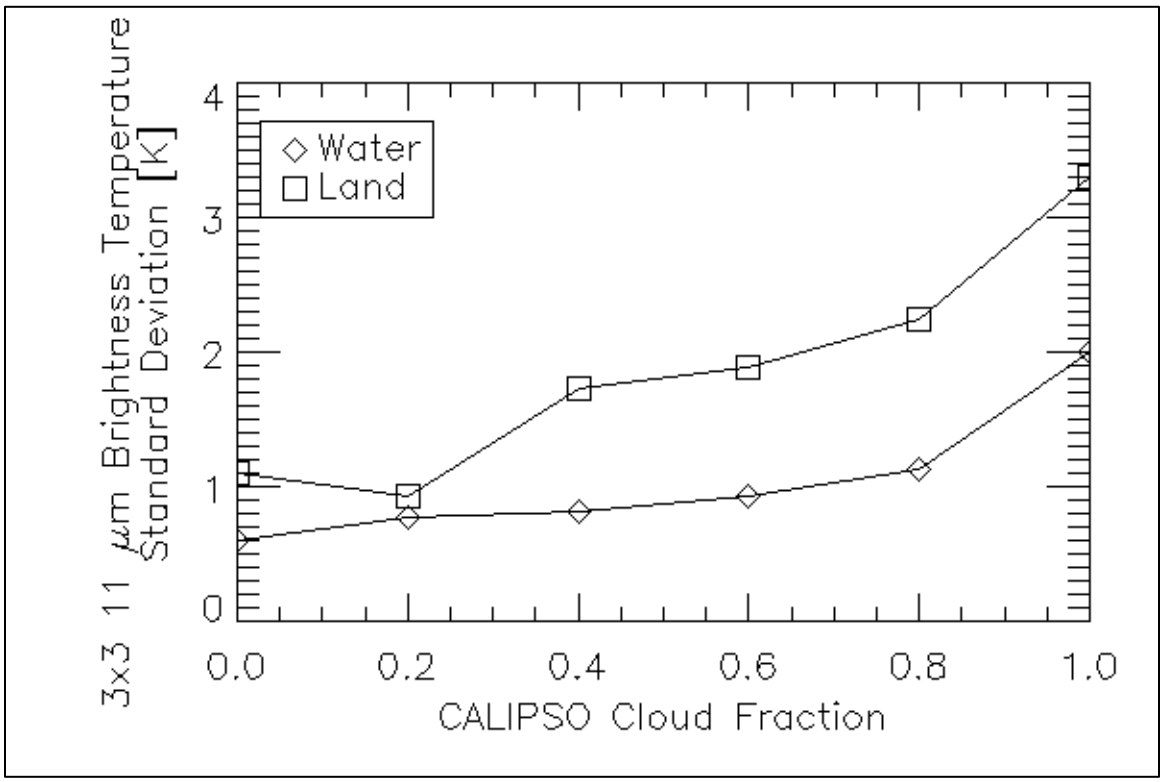

Figure 5. Variation of the standard deviation of the 11 μm brightness temperature computed over a 3x3 pixel array as a function of the CALIPSO cloud fraction.

In the ECM, the 11-12 BTD positive values are used to detect the presence of semi-transparent cloud. This classifier represents the difference between the observed 11-12 BTD and an estimate of the clear-sky value that is consistent with the observed 11-μm brightness temperature. When the 11-μm clear-sky brightness temperature falls below 265 K, the classifier is set to 11-12 BTD. The goal of this formulation is to bring in information from the clear-sky model to make the classifiers account for variations in surface temperature and atmospheric moisture.

3.4.1.4.6 11 and 6.7 μm Thermal Contrast Test (BTD11_6.7)

The logic of this test is based on the difference of the waiting function for 11 and 6.7 μm channels. 6.7 μm is in water vapor absorption band, and provides good sensitivity to the relatively cold regions of the atmosphere. However, this test is off for pixels with BT11 less than 220K. The brightness temperature difference of these channels test is developed for catching thin clouds.

3.4.1.4.7 11 and 6.7 μm Thermal Covariance Test (BT11_BT6.7Covar)

This test is using covariance from 5x5 pixel boxes of 11 and 6.7 μm brightness temperatures. Because 6.7 μm never sees the ground over cloudy pixels BTs of both

channels change together (high covariance), and opposite is true for clear pixels when 11 μm would see the ground BTs are changing not together (low covariance). The 11 and 6.7 μm covariance is an input to the ECM.

3.4.1.4.8 11 and 8.5 μm Thermal Contrast Test (BTD11_8.5)

Similar to BTD11_6.7 the logic of this test is based on the difference of the waiting function for 11 and 8.5 μm. Less than zero BTD11_8.5 is indicating cloud, while positive difference, over oceans, indicates clear regions. As atmospheric moisture increases, BTD11_8.5 increases. In Polar Regions during winter, large positive values in BTD11_8.5 during winter time over the Antarctic Plateau and Greenland indicate a strong surface inversion and thus clear skies.

3.4.1.4.9 Daytime 4 μm Emissivity Test (EMISS4_Day)

The 4μm emissivity test exploits the very high sensitivity of 4 μm observations to the presence of cloud. For some sensors ECM uses 3.75 μm. Cloud detection tests in the 4 μm region often use brightness temperature differences computed from the 4 μm brightness temperature and the 11 or 12 μm brightness temperatures. The ECM employs the 4 μm emissivity, (e_4) which is computed using the following relationship.

$$e_4 = I_4 \Big/ I_{4,bb} \tag{23}$$

where I_4 is the 4μm observed radiance and $I_{4,bb}$, the 4μm blackbody radiance, which is calculated by substituting the 11 μm brightness temperature into the Planck function, while using the appropriate coefficients for the 4 μm channel. The EMISS4 test uses the following metric (χ) in the test:

$$\chi = (e_4 - e_{4,clear}) \Big/ e_{4,clear} \tag{24}$$

The value of $e_{4,clear}$ is an estimate of e_4 under cloud-free conditions and is an input to the ECM.

This particular metric was chosen to make a cloud detection test using the 4 μm channel that is largely insensitive to the solar viewing geometry. One of the main disadvantages of brightness temperature difference tests are that the observed values are impacted greatly by the solar geometry and the scene temperatures. Applying a constant brightness temperature threshold would therefore offer different sensitivity to the presence of cloud over different regions and times of day. This formulation does not remove the ambiguity that occurs in the 4 μm radiances during terminator conditions where the contribution of the observed radiance due to reflected sunlight is comparable to that due to emission. Because of that, the EMISS4_Day test is not applied in the glint regions as determined by the derived glint mask. In addition, if the pixel is to warm (an 11 micron BT of 310), this test isn't performed.

3.4.1.4.10 Nighttime 4 μm Emissivity Test (EMISS4_Night)

This classifier also uses 4μm pseudo emissivity. Without solar illumination, the 4 micron emissivity for low opaque clouds can fall well below unity. For semitransparent and cold cloud, the 4 μm emissivity becomes very large. There is no need for solar zenith angle scaling as in the daytime classifier. The ranges of the day and night *e4* values were different enough to warrant separate classifiers to improve performance. The nighttime 4-micron pseudo emissivity classifier is defined as the value of *e4* without any scaling. Figure 4 shows the variation of the nighttime 4-micron pseudo emissivity metric given in Equation 23. For visual convenience, the nighttime values of *e4* plotted in Figure 4 are offset by 1. The variation of nighttime and daytime 4 μm pseudo emissivity metrics are qualitatively similar for ice clouds as illustrated in Figure 4. For water clouds, the nighttime metric can fall below the clear-sky values and for this reason; the nighttime and daytime classifiers are separated.

3.4.1.4.11 Night 4 and 11 μm Thermal Contrast Test (BTD4_11)

Another similar to BTD11_6.7 and BTD11_8.5 logic is BTD4_11 test. It calculates the difference between 4 and 11 μm brightness temperatures. During the nighttime positive values of BTD4_11 are used to detect partial clouds or thin clouds within the sensor field of view. Negative differences occur over extended clouds due to the lower cloud emissivity at 4 μm.

3.4.1.4.12 0.63 μm Reflectance (Ref0.63)

The 0.63-micron reflectance is very important in cloud detection owing to the high reflectivity of clouds and relatively low reflectivity of most surface types. This classifier is the difference between observed 0.63-micron reflectance and the estimated value under cloud-free conditions. At night if available, the lunar reflectance is used. The clear-sky estimate is generated using the surface reflectance maps described by Moody et al. (2007) coupled with a Rayleigh and aerosol scattering model (see Section 1.9.3.4). While inclusion of this test is contrary to prioritization of the IR channels, it is necessary to maintain consistent performance during daytime periods. This test is off over glint, mountain, and forward scattering angles.

3.4.1.4.13 Relative Visible Contrast Test (RVCT)

The basic premise of the RVCT is that over a small region pixels that are much brighter than the darkest pixel in the neighborhood are likely cloudy. The RVCT metric used in the ECM is the observed 0.63 μm reflectance minus the minimum value observed over a 3x3 pixel array centered on the pixel being tested. At night if available, the lunar reflectance is used. The targeted cloud features of the RVCT are small scale clouds and cloud edges. However, care must be exercised to avoid the false detection of cloud in the presence of coasts and other strong surface reflectance gradients. Therefore the test is not applied over known snow/ice surfaces (based on ancillary data) or coastal and mountain regions, as the variability in the surface reflectance is too great. The benefit of this test is that it is not dependent on knowledge of the surface reflectance.

3.4.1.4.14 0.63 μm Reflectance Uniformity Test (Ref0.63STD)

This test is similar to BT11STD, it compares standard deviation of 0.63 μm reflectance over 3x3 pixel box during the day time. At night if available, the lunar reflectance is used. The pixel is defined cloudy if it has high variability (STD), and clear for low STD. The physical basis is the assumption that clear regions should exhibit relatively spatially uniform reflectivity over land and ocean. Because of the non-uniformity of coasts and snow, this test is not applied on those pixels. This test is used for cloud ages over water and land, but can't be used over coastal and mountain regions.

In the ECM, the Ref0.63STD is applied to the 0.63 μm reflectance standard deviation computed over a 3x3 pixel array for daytime pixels with solar zenith angles out to 80.0 degrees. Figure 6 shows the variation of this quantity for land and ocean pixels plotted as a variation of the collocated CALIPSO cloud fraction. As stated above, the goal of this test is to separate truly clear pixels from those that are cloud contaminated. This analysis shows that the Ref0.63STD, as formulated here, is indeed insensitive to the underlying surface reflectance.

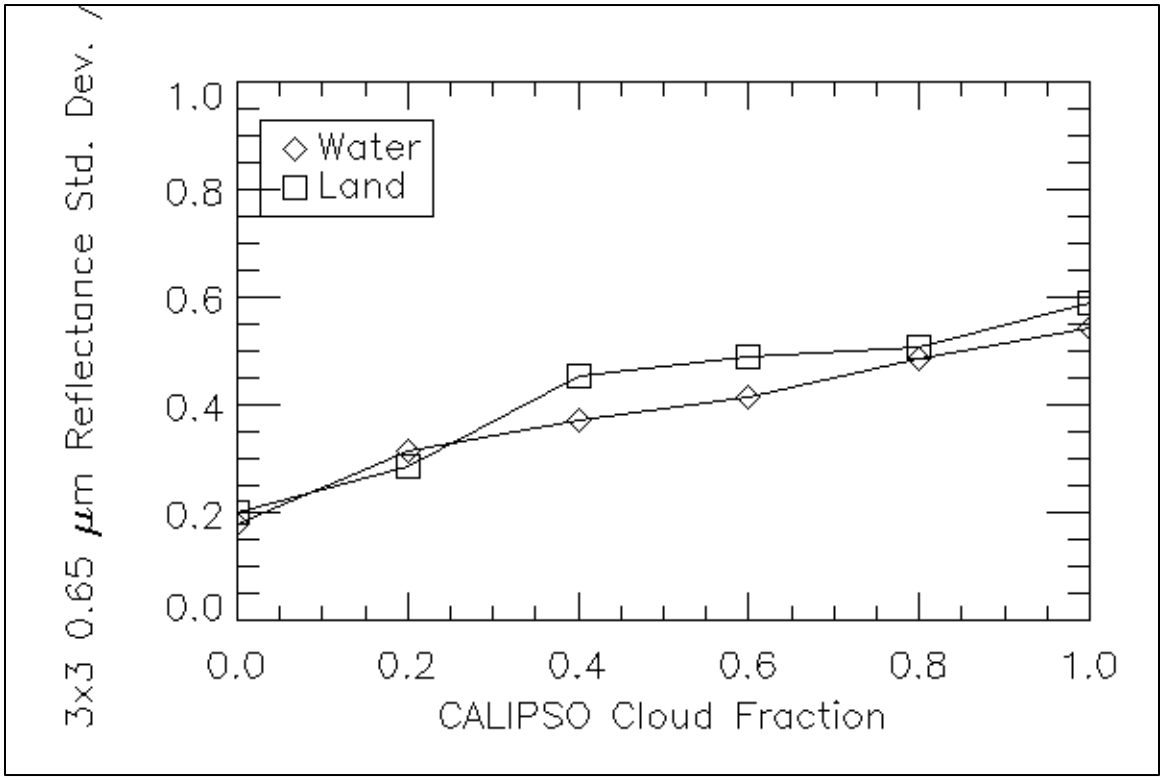

Figure 6. Variation of the standard deviation of the 0.65 μm reflectance computed over a 3x3 pixel array as a function of the CALIPSO cloud fraction.

3.4.1.4.15 Reflectance Ratio Test (Ref_Ratio)

This test utilizes ratio of the reflectances from 0.63 and 0.86 μm channels. This test makes use of the fact that the spectral reflectance at these two wavelengths is similar over

clouds (ratio is near 1) and different over water and vegetation. It is off over mountains (surface elevation of over 2000m), glint, and terminator (solar zenith angle greater than 85 degrees).

3.4.1.4.16 1.38 μm Reflectance Test (Ref1.38)

The 1.38 μm channel on MODIS has been used successfully to detect thin cirrus (Ackerman et al., 2002). The 1.38 μm channel resides in a strong water vapor absorption band that masks the surface under most conditions. The test is applied to all pixels that have a solar zenith angle of less than 80^o, that are not in surface height, with a maximum surface height of less than 2000m, and are not snow or Antarctic pixels.

3.4.1.4.17 NDSI Test (NDSI)

Due to significant differences in the imaginary indices of the refraction index of water and ice in some regions of the near-infrared (NIR) spectrum, NIR reflectances are useful for detecting water cloud on top of snow and ice covered surfaces. The NIR channels, particularly the 1.6μm reflectance are useful in discriminating between snow and clouds, as snow has very low 1.6μm reflectance, while the 1.6μm reflectance of clouds remains high. Consequently, both cirrus and optically thick water clouds can be directly classified and distinguished from snow using the 1.6μm channel (Warren, 1982). In fact, the usefulness of the 1.6μm channel has been demonstrated on both the operational Landsat Thematic Mapper satellite (Dozier, 1989; Baglio, 1989) as well as the AVHRR instrument. In addition, because of the strong signal of snow in the 1.6μm reflectance, it is also used to calculate the Normalized Difference Snow Index (NDSI). Thus, the 1.6μm reflectance is a useful test for clouds over snow.

Should the 1.6 μm reflectance not be available and the 3.9 μm reflectance is available, this test can also use the 3.9 μm reflectance.

However, there are some drawbacks to this test, such as prior knowledge of which pixels contain snow and which are snow-free, information provided by the snow mask described in Section 1.9.2. In addition, there are issues at surface elevations (over 1000 m) as well as coastal pixels, as defined by the coast mask; thus, this test is not performed in these areas. Finally, this test cannot be performed in high solar zenith angle regions.

For options, each pixel is tested to see if the pixel is snow, has a solar zenith angle of less than 80^o and a surface height of less than 1000m.

If the test uses the 1.6 μm reflectance, the NDSI is then calculated

$$NDSI = \frac{R_{0.64} - R_{1.6}}{R_{0.64} + R_{1.6}} \tag{25}$$

where $R_{0.64}$ is the 0.64 μm reflectance and $R_{1.6}$ is the 1.6 μm reflectance.

3.4.2 Algorithm Output

The following section describes the three sets of output from the ECM algorithm.

3.4.2.1 Output

The final output of the ECM consists of a 4-level cloud mask. The cloud mask values and a description of their meaning are given below in Table 3. The initial value for the ECM is -128.

Table 3. Cloud mask values and their descriptions

Cloud Mask Value	Numerical Value	Description
Clear	0	Cloud probability ≤ 0.1
Probably Clear	1	Cloud probability > 0.1, but ≤ 0.5
Probably Cloudy	2	Cloud probability > 0.5, but ≤ 0.9
Cloudy	3	Cloud probability > 0.9

The algorithm also produces 7 bytes (Table 4) of output which are comprised of bits holding the test results for each of the various tests and flags that are used to compute the cloud probability (0.0 – 1.0) and final 4-level cloud mask product (Table 3), and are required inputs for other algorithms.

Table 4. Cloud mask tests and flags and their descriptions.

Byte	Bit	Flag Description Key	Result
0	0	Cloud Mask Attempted Flag	1 = Yes 0 = No
	1	Daytime Visible Tests Attempted	1 = Yes 0 = No
	2	Daytime Spatial Uniformity Tests Attempted	1 = Yes 0 = No
	3	4 μm Daytime Tests Attempted	1 = Yes 0 = No
	4	4 μm Nighttime Tests Attempted	1 = Yes 0 = No
	5	Solar Contamination Flag	1 = Yes 0 = No
	6	Coast / No Coast Flag	1 = Yes 0 = No
	7	Mountain / No Mountain Flag	1 = Yes 0 = No
1	0	Forward Scattering Flag	1 = Yes 0 = No
	1	3.75 μm Cold Scene Flag	1 = Yes 0 = No
	2	11 μm Cold Scene Flag	1 = Yes 0 = No
	3	Oceanic Glint Flag	1 = Yes 0 = No
	4	Smoke Contamination Flag	1 = Yes 0 = No
	5	Dust Contamination Flag	1 = Yes 0 = No
	6	Shadow Contamination Flag	1 = Yes 0 = No
	7	Fire Contamination Flag	1 = Yes 0 = No
2	0-2	Surface Type Used for Thresholds	000 = Deep Ocean 001 = Shallow Water 010 = Land

			011 = Snow 100 = Arctic 101 = Antarctic + Greenland 111 = Desert
	3	SPARE	
	4-5	BT11 – 11 μm Thermal Test	00 = Clear 01 = Probably Clear 10 = Probably Cloudy 11 = Cloudy
	6-7	RTCT – Relative Thermal Contrast Test	00 = Clear 01 = Probably Clear 10 = Probably Cloudy 11 = Cloudy
3	0-1	BT11STD – 11μm Thermal Uniformity Test	00 = Clear 01 = Probably Clear 10 = Probably Cloudy 11 = Cloudy
	2-3	ETROP – Emissivity at Tropopause Test	00 = Clear 01 = Probably Clear 10 = Probably Cloudy 11 = Cloudy
	4-5	BTD11_12 – 11 and 12 μm Split-Window Test	00 = Clear 01 = Probably Clear 10 = Probably Cloudy 11 = Cloudy
	6-7	BTD11_6.7 – 11 and 6.7 μm Thermal Contrast Test	00 = Clear 01 = Probably Clear 10 = Probably Cloudy 11 = Cloudy
4	0-1	BTD11_6.7 – 11 and 6.7 μm Thermal Covariance Test	00 = Clear 01 = Probably Clear 10 = Probably Cloudy 11 = Cloudy
	2-3	BTD11_8.5 – 11 and 8.5 μm Thermal Contrast Test	00 = Clear 01 = Probably Clear 10 = Probably Cloudy 11 = Cloudy
	4-5	EMISS4 – 4 μm Emissivity Test	00 = Clear 01 = Probably Clear 10 = Probably Cloudy 11 = Cloudy
	6-7	EMISS4 _Day – Daytime 4 μm Emissivity Test	00 = Clear 01 = Probably Clear 10 = Probably Cloudy 11 = Cloudy

5	0-1	EMISS4 _Night – Nighttime 4 μm Emissivity Test	00 = Clear 01 = Probably Clear 10 = Probably Cloudy 11 = Cloudy
	2-3	SPARE	
	4-5	Ref0.63 – 0.63 μm Reflectance Test	00 = Clear 01 = Probably Clear 10 = Probably Cloudy 11 = Cloudy
	6-7	Ref0.63STD – 0.63 μm Reflectance Uniformity Test	00 = Clear 01 = Probably Clear 10 = Probably Cloudy 11 = Cloudy
6	0-1	RVCT – Relative Visible Contrast Test	00 = Clear 01 = Probably Clear 10 = Probably Cloudy 11 = Cloudy
	2-3	Ref_Ratio – Reflectance Ratio Test	00 = Clear 01 = Probably Clear 10 = Probably Cloudy 11 = Cloudy
	4-5	Ref1.38 – 1.38 μm Reflectance Test	00 = Clear 01 = Probably Clear 10 = Probably Cloudy 11 = Cloudy
	6-7	NDSI – NDSI Test	00 = Clear 01 = Probably Clear 10 = Probably Cloudy 11 = Cloudy

The following bits: smoke, dust, shadow and fire are added as an extra to the ECM. The smoke and dust detection are implemented from the VCM algorithm and fully described in JPSS VCM ATBD, and are calculated only for VIIRS. The smoke, dust and fire bits use information from the I1 (0.64 μm), I4 (3.74 μm) and I5 (11 μm) channels. The shadow algorithm is simply based on geometrical calculations of cloud height, location, and angular location of the sun. The fire detection is implemented from current operational EUMETSAT algorithm and described in Joro et al., 2008.

3.4.2.2 Metadata

In addition to the algorithm output and quality flags, the following will be output to the file as metadata for each file:

- Percent of pixels that are clear, probably clear, probably cloudy, and cloudy
- Number of cloud mask categories (4 cloud mask categories: Clear, Probably Clear, Probably Cloudy and Cloudy)
- For each cloud mask category, the following information is required:
    - Count of pixels for the cloud mask category

    - Definition of cloud mask category
- Total number of cloud mask points.
- Terminator mark or determination.
- Minimum, Maximum and Mean observation-calculation for all-sky (IR Channels).
- Minimum, Maximum and Mean observation-calculation for clear-sky (IR Channels).
- Standard deviation between observation and calculation for all-sky (IR Channels).
- Standard deviation between observation and calculation for clear-sky (IR Channels).

4 Test Data Sets and Outputs

4.1 Input Datasets

As described below, the data used to test the ECM included VIIRS observations collocated with CALIPSO data and with MODIS granules. These validation data sets used in assessing the performance of the ECM.

4.1.1 VIIRS Data

VIIRS provides 16 M-Band spectral channels with a nadir spatial resolution of 750 m. The Figure 7, shown below, is aggregated images from 2030 UTC to 2040 UTC on June 01, 2015. On the left it is a true color image of Hurricane Andres, and on the right – corresponding 4-level ECM result.

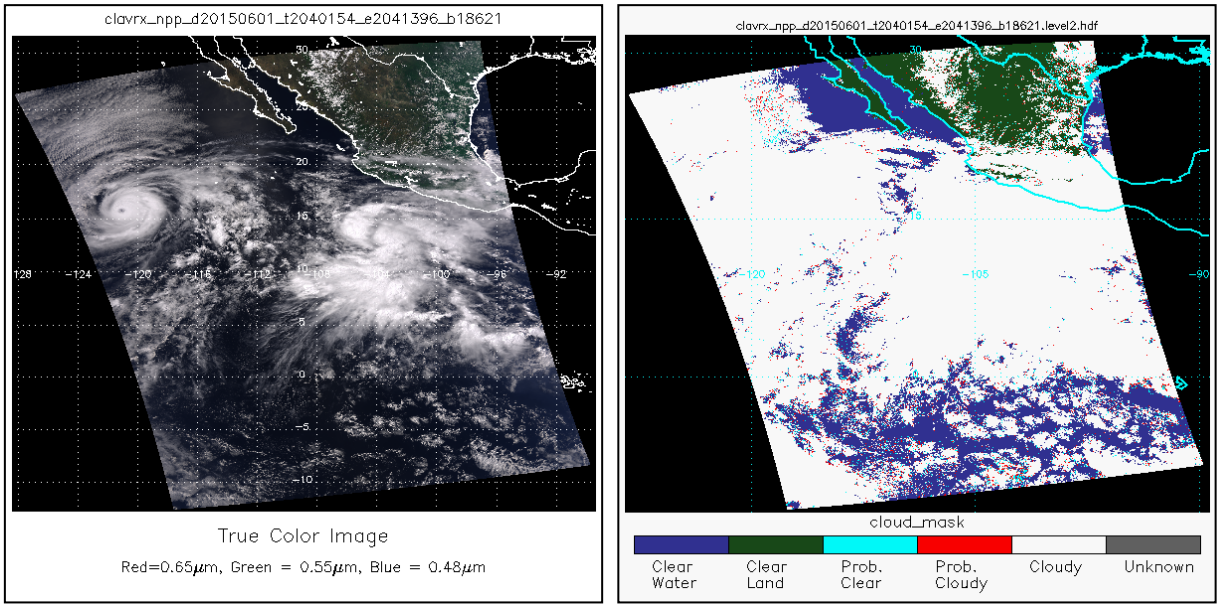

Figure 7. Aggregated images of 8 SNPP VIIRS granules of Hurricane Andres on 06/01/2015 from 2030UTC to 2040UTC (left - True Color RGB, right - NOAA Enterprise Cloud Mask).

4.1.2 CALIPSO Data

With the launch of CALIPSO and CloudSat into the Earth Observing System (EOS) A-Train in April 2006, the ability to conduct global satellite cloud product validation increased significantly. Currently, CALIPSO cloud detection results are used to train and validate the cloud detection of the ECM. The CALIPSO data used here are the 1 km cloud layer results (Vaughan et al., 2005).

Figure 8 shows a collocation example of CALIPSO and one GOES-15 granule from June 01, 2015 at 21.00UTC. Accuracy of the cloud mask detection retrieved from this GOES granule is 93% in comparison to CALIPSO observations.

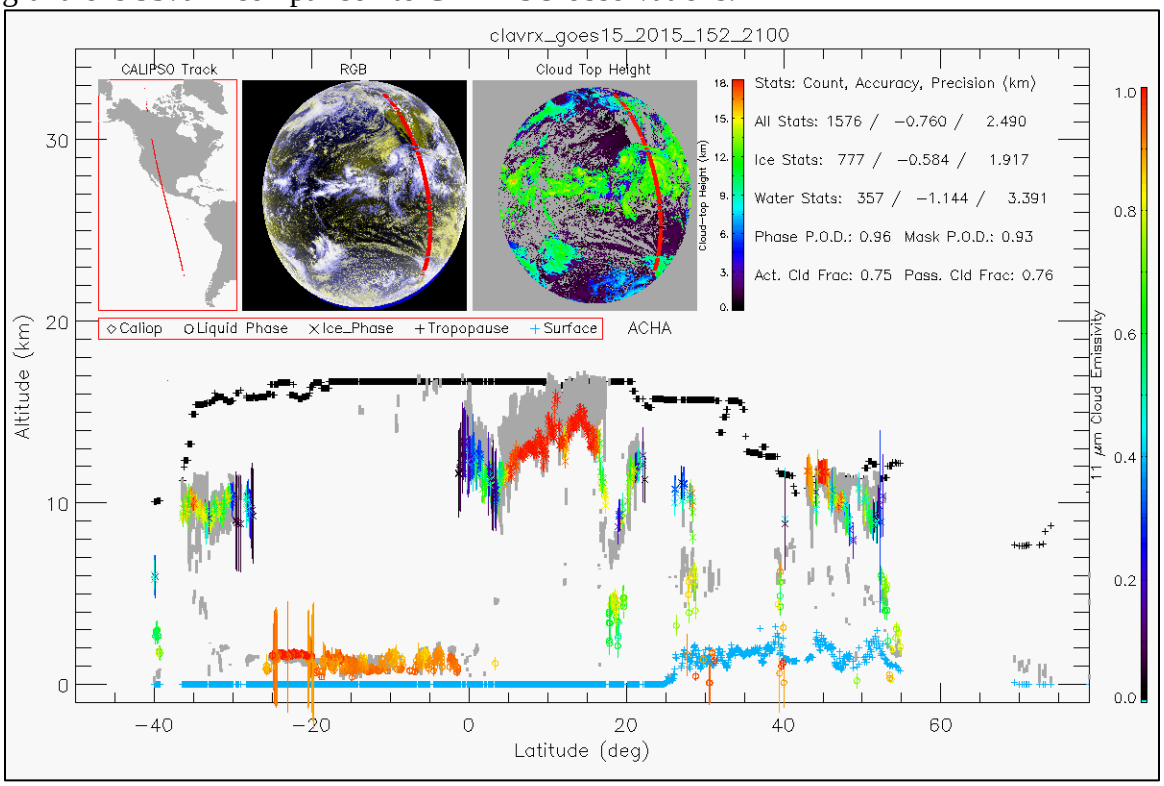

Figure 8. A collocation example of GOES-15 and CALIPSO is from June 01, 2015 at 21.00UTC (Hurricane Andres case). The upper panel of the figure shows the CALIPSO track, RGB image, the retrieved cloud top height, and some statistics. The lower panel shows cloud height along the CALIPSO track. Gray shaded areas indicate CALIPSO profiles. Colored symbols and lines show ACHA results and uncertainty estimates.

The individual CALIPSO results within each GOES pixel were averaged to give a cloud fraction for each VIIRS pixel. This cloud fraction is compared to the 4-level ECM results. The error is estimated as the percentage of pixels for each cloud mask category that falls outside the following ranges of CALIPSO cloud fraction: the requirements state that this is a “Clear-sky” mask, and as such, the probably clear and clear pixels are called “Clear” and probably cloudy and cloudy pixels are called “Cloud.” In addition, for the analysis with CALIPSO, only cloud fractions equal to 100% were considered as cloud while all other conditions were considered clear pixels by CALIPSO.

The distribution of clouds CALIPSO detects can be seen on Figure 9. On the X axes it is cloud emissivity computed from the MODIS 11 μm radiances and the clear-sky radiances assuming the cloud existed at the height given by CALIPSO. It is in bins with 0.2 width and ranges from -0.2 to 1.2. On the Y axes height bins are set to a width of 2 km thick and range from 0 to 16 km. Emissivity less than 0 imply the observed radiance was less

than the clear-sky radiance, and emissivities greater than 1.0 imply that the observed radiance was greater than the blackbody emission at the CALIPSO cloud temperature. Mostly CALIPSO detects thin cirrus at the height around 10 km and emissivity of 1.

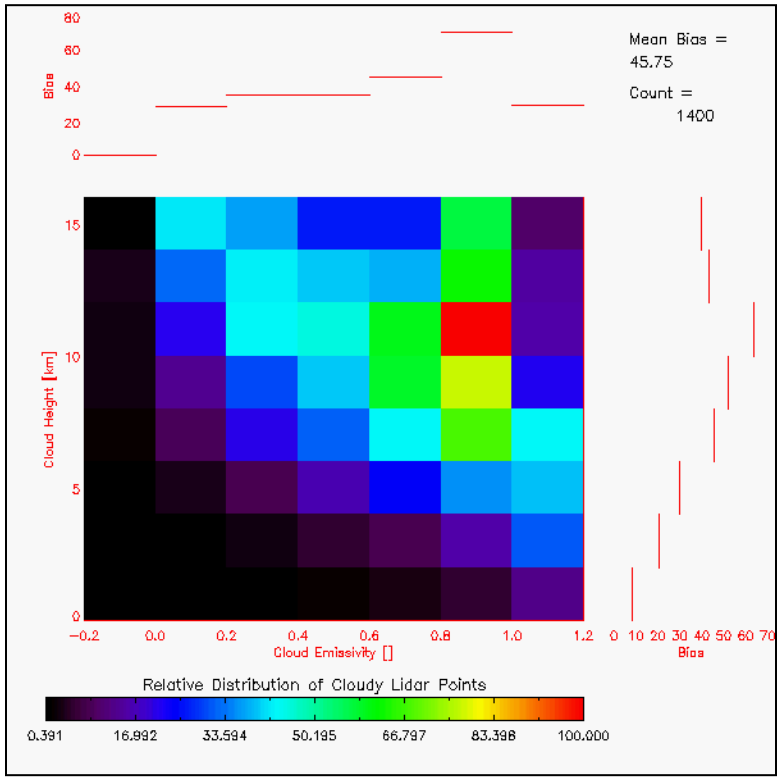

Figure 9. CALIPSO cloud detection distribution of all collocated (CALIPSO-MODIS) pixels in height and cloud top emissivity.

4.1.3 Precisions and Accuracy Estimates

To estimate the performance and accuracy of the ECM, we have used the MODIS Cloud Mask product (MOD35/MYD35) and CALIPSO data as described above. This section will present our analysis methodology for estimating the precision and accuracy. The next section will provide the quantitative results in terms of the L1RDS specifications.

4.1.3.1 CALIPSO Analysis

The CALIPSO/CALIOP data (hereafter referred to as CALIPSO) provides unique information on the cloud fraction, which can be used to validate the ECM. To do this analysis, a collocation tool has been developed to determine the relevant information provided by CALIPSO for each collocated MODIS and VIIRS pixel. This tool has been applied to all MODIS data for the datasets specified in this Section. For each pixel that is collocated with CALIPSO data, the following information is available.

- Time difference between passive sensor and CALIPSO

- Number of cloud layers observed by CALIPSO
- Cloud fraction

The analysis shown in this section provides the performance of the ECM based on cloud height (Z_c) and emissivity (e_c) as provided by CALIPSO. The height and emissivity bins are set exactly as in Figure 9.

Figure 10 is the distribution in Z_c-e_c space of the clouds detected by CALIPSO that were missed by the ECM. The values in Figure 10 show the fraction of missed clouds computed from the number of missed clouds divided by the total number of cloudy pixels in each Z_c-e_c bin. This analysis reveals that the ECM performs well for all clouds with e_c > 0.2. The probability of correct detection (POD) for the binary ECM results compared to CALIPSO. False cloud is the percentage of falsely detected cloud pixels while false clear is the percentage of falsely detected clear pixels. The L1RDS requirements (Table 1) account only for clouds with cloud optical depth > 1.0, we did not use this filter in this analysis. However, ECM results show probability of detection is 94%, probability of missed clouds 1%, and probability of false cloud is 4%.

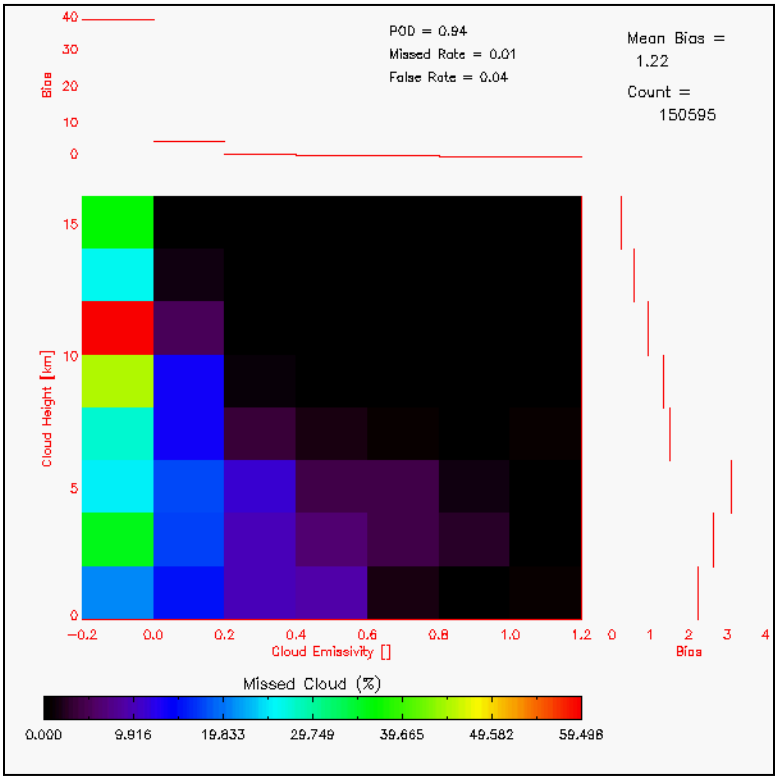

Figure 10. CALIPSO-derived height and emissivity distribution of pixels that were cloudy as observed by CALIPSO but classified as clear by the ECM. Values are fractions of missed cloudy pixels over the total number of CALIPSO-derived cloudy pixels in each Zc-ec bin. Light gray indicates no data.

Figure 11 shows location of 3 days of collocation pixels between VIIRS – CALIPSO on the left, and MODIS – CALIPSO on the right (08/14/2012, 11/10/2012 and 02/09/2013). Daytime pixels are indicated in blue color, while nighttime in red. Table 5 shows the statistical comparison for the binary ECM, VCM and MODIS C6 cloud masks results compared to CALIPSO.

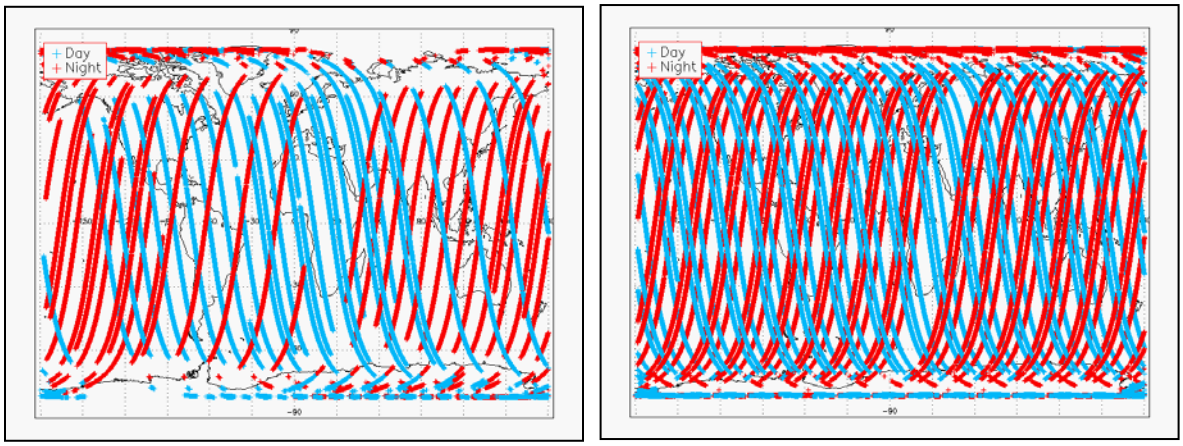

Figure 11. Location of the collocated pixels for VIIRS – CALIPSO (left) and MODIS – CALIPSO (right) for 3 days (08/14/2012, 11/10/2012 and 02/09/2013). Blue crosses for daytime, red – nighttime.

The number of correct cloud decisions is computed as the number of pixels where Cloud Mask algorithms gave a cloudy results and the CALIPSO cloud fraction was greater than 0.8. The number of correct clear decisions was computed as the number of pixels where algorithms gave a clear decision and the CALIPSO cloud fraction was less than 0.2

Table 5. Cloud Mask Algorithms comparison for VIIRS – CALIPSO and MODIS – CALIPSO collocated pixels from Figure 11. Applied filters are indicated in the table.

Cloud Mask Algorithm	Sample Size	Cloud fraction				Probability of		
		Active	Passive	Pr. Clear	Pr. Cloudy	Detection	False D.	Miss Cld.
90N – 90S, Ocean/Land, Day/Night, No Snow/Snow/Ice								
NOAA ECM VIIRS	901051	0.715	0.697	0.054	0.060	0.909	0.037	0.054
VCM IDPS	860046	0.716	0.641	0.071	0.031	0.878	0.024	0.099
NOAA ECM MODIS	1222722	0.727	0.698	0.060	0.050	0.927	0.022	0.051
MODIS C6	1222722	0.727	0.707	0.061	0.044	0.926	0.027	0.047
60N – 60S, Ocean/Land, Day/Night, No Snow/No Ice								
NOAA ECM VIIRS	729886	0.713	0.684	0.035	0.033	0.928	0.022	0.051
VCM IDPS	690211	0.715	0.659	0.069	0.030	0.911	0.017	0.072
NOAA ECM MODIS	876514	0.715	0.689	0.028	0.025	0.954	0.010	0.036
MODIS C6	878574	0.716	0.707	0.074	0.035	0.950	0.021	0.029

All algorithms show a very good performance with POD more than 90%, except VCM global number is 87.8%.

4.1.3.2 MODIS Analysis

As stated above, CALIPSO provides our source of cloudiness information that is used to derive and verify the ECM. To complement the CALIPSO analysis, the ECM was also compared to the official NASA Goddard MODIS cloud mask, which is also known as MYD35 Collection 6 (Ackerman et al., 1988; Ackerman et al., 2002). The MYD35 C6 provides a 4-category cloud mask at a spatial resolution of 1 km. It has become a widely-used cloud mask for many MODIS applications.

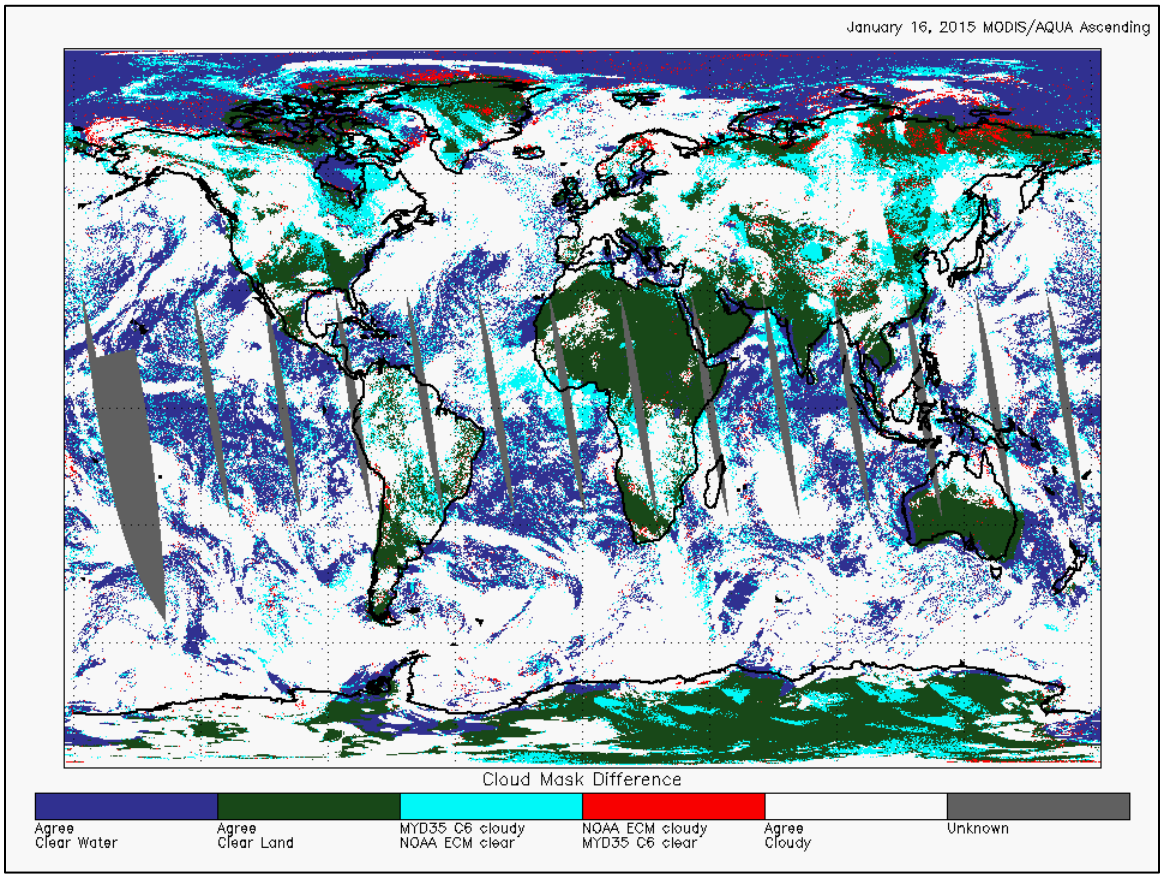

Figure 12. Comparison of MODIS (MYD35 C6) and the ECM applied to MODIS data on January 16, 2015 (ascending mode).

To compare the ECM results to MODIS, the ECM was processed through using MODIS granules for a single day. Because the input to the ECM for this analysis was the MODIS imagery, the analysis was able to compare the MYD35 output and the output of the ECM directly. Figure 12 shows a direct comparison of the ECM applied to MODIS as compared to the MYD35 C6 results. Regions that are white represent regions where both MYD35 C6 and the ECM gave cloudy results. Regions that are blue or green represent

areas where both MYD35 C6 and the ECM gave clear results. Regions that are red are those where MYD35 C6 gave clear results and the ECM gave a cloudy result. Finally, cyan regions are those where the ECM detected clear and the MYD35 C6 did not. There does appear to be a general preference for the ECM to detect less cloud than MYD35 C6 in the presence of sun glint and over snow surfaces. The zonal cloud fractions are also in rough agreement with ECM a little bit smaller (not shown). While this was just a single day, the results covered a wide range of conditions and land types.

In summary, while any passive satellite product cannot be considered a source of validation for another passive satellite product, the MYD35 C6 comparison does provide evidence that the ECM is performing well and as expected.

5 Practical Considerations

5.1 Numerical Computation Considerations

The ECM is implemented sequentially. Because some cloud detection tests rely on the values of the ancillary data flags, the ancillary data flags need to be computed first. All tests are applied before the final cloud mask is determined. The ECM is currently implemented into the Enterprise system and uses its numerical routines for processing.

5.2 Programming and Procedural Considerations

The ECM requires knowledge of spatial uniformity metrics that are computed for each pixel using pixels that surround it. Beyond this reliance, the ECM is purely a pixel by pixel algorithm.

5.3 Quality Assessment and Diagnostics

The following procedures are recommended for diagnosing the performance of the ECM.

- Monitor the percentage of pixels falling into each ECM cloud mask values. These values should be quasi-constant over a large area.
- Derive a surface temperature from all clear pixels of the ECM. Compute the distributions of the observed – background surface temperature for each ECM clear value.
- Periodically image the individual test results to look for artifacts or non-physical behaviors.
- Maintain a close collaboration with the other teams using the ECM in their product generation.

5.4 Exception Handling

The ECM includes checking the validity of each channel before applying the appropriate test. The ECM also expects the main processing system (i.e., the Enterprise) to flag any pixels with missing geolocation or viewing geometry information.

The ECM does check for conditions where the ECM cannot be performed. If the 11 μm channel measured or clear sky BT is saturated or missing, there is no attempt at processing the cloud mask, as it is a key channel in numerous tests for the ECM. If other channels are saturated or missing, the corresponding tests are not performed. A quality flag is set, which indicates the quality of the cloud mask for that particular pixel. The conditions for the quality flags are described in Section 1.10.2.1.

6 ASSUMPTIONS AND LIMITATIONS

The following sections describe the current limitations and assumptions in the current version of the ECM.

6.1 Performance

The following assumptions have been made in developing and estimating the performance of the ECM. The following list contains the current assumptions and proposed mitigation strategies.

1. NWP data of comparable or superior quality to the current 6 hourly GFS forecasts are available. (Use longer range GFS forecasts or switch to another NWP source – ECMWF).

2. RTM calculations are available for each pixel. (Use reduced vertical or spatial resolution in driving the RTM).

3. High quality snow maps are available. (Use snow information from NWP).

4. Background snow-free surface reflectances will be available. (Use precomputed reflectances stored as function of surface type).

5. All of the static ancillary data is available at the pixel level. (Reduce the spatial resolution of the surface type, land mask and or coast mask).

6.2 Assumed Sensor Performance

The ECM is dependent on the following instrumental characteristics:

- The spatial uniformity tests in ECM will be critically dependent on the amount of striping in the data.
- Unknown spectral shifts in some channels will cause biases in the clear-sky RTM calculations that may impact the performance of the ECM.

6.3 Pre-Planned Product Improvements

This section contains the potential future enhancements to the algorithm, the limitations they will mitigate, and possible and useful related information and links.

The ECM serves many other applications. Its development is therefore tied to the development and feedback from the other algorithms. At this point, it is therefore difficult to predict what the future modifications will be. However, the following list contains our current best guess of the future ECM modifications.

6.3.1 Optimization for Ocean Applications

The cloud detection accuracy requirements of the SST and aerosol applications over the ocean are very strict. It is recognized that specialized tests for these applications will be necessary. Coordination with the Ocean Application Team regarding the ECM algorithm and output is being done to incorporate their experience and to ensure the ECM is adequate for their needs.

6.3.2 Optimization for Land Applications

The ECM performance over land also needs to be optimized for the Land Application Team's algorithms. Coordination with the Land Application Team regarding the ECM algorithm and output is being done to allow for their feedback and to ensure the ECM is adequate for their needs.

7 REFERENCES

Ackerman, S.A., K.I. Strabala, W.P. Menzel, R.A. Frey, C.C. Moeller and L.E. Gumley, 1998: Discriminating clear sky from clouds with MODIS. J. Geophys. Res., **103**, 32139-32140.

Ackerman, S. A., Strabala, K. I., Menzel, W. P., Frey, R. A., Moeller, C. C., Gumley, L. E., Baum, B., Wetzel-Seeman, S., and Zhang, H.: Discriminating clear sky from clouds with MODIS Algorithm Theoretical Basis Document (MOD35), Tech. Rep. ATBD-MOD-06, University of Wisconsin-Madison, 2002

Baglio, J.V., and Holroyd, E.W., 1989. Methods for operational snow cover area mapping using the advanced very high resolution radiometer: San Juan Mountains Test Study, Research Technical Report, U.S. Geological Survey, Sioux Falls and U.S. Bureau of Reclamation, Denver.

Derrien M., and H. Le Gleau, MSG/SEVIRI cloud mask and type from SAFNWC, International Journal of Remote Sensing 26 (2005), pp. 4707–4732.

Dozier, J., 1989. "Remote sensing of snow in visible and near-infrared wavelengths," Theory and Applications of Optical Remote Sensing, G. Asrar, ed., John Wiley and Sons, New York.

Dybbroe, A., K.G. Karlsson, and A. Thoss, 2005: NWCSAF AVHRR Cloud Detection and Analysis Using Dynamic Thresholds and Radiative Transfer Modeling. Part I: Algorithm Description. *J. Appl. Meteor.*, **44**, 39–54.

Dybbroe, A., K.G. Karlsson, and A. Thoss, 2005: NWCSAF AVHRR Cloud Detection and Analysis Using Dynamic Thresholds and Radiative Transfer Modeling. Part II: Tuning and Validation. *J. Appl. Meteor.*, **44**, 55–71.

GOES-R Series Ground Segment (GS) Project Functional and Performance Specification (F&PS) [G417-R-FPS-0089]

GOES-R Level 1 Requirements Document (L1RD)

GOES-R Series Mission Requirements Document (MRD) [P417-R-MRD-0070]

GOES-R Acronym and Glossary (P417-R-LIST-0142)

GOES-R Algorithm Interface and Ancillary Data Description Document (AIADD)

Hann, S. L. L. Strow, and W. W. McMillan, 1996: Atmospheric infrared fast transmittance models: A comparison of two approaches, Proceedings of SPIE, 2830, 94-105.

Hansen, M., R. DeFries, J.R.G. Townshend, and R. Sohlberg (1998), UMD Global Land Cover Classification, 1 Kilometer, 1.0, Department of Geography, University of Maryland, College Park, Maryland, 1981-1994.

Heidinger, Andrew K.; Evan, Amato T.; Foster, Michael J. and Walther, Andi.: A naive Bayesian cloud-detection scheme derived from CALIPSO and applied within PATMOS-x. Journal of Applied Meteorology and Climatology, Volume 51, Issue 6, 2012, 1129–1144

Heidinger, Andrew K.; Frey, Richard and Pavolonis, Michael.: Relative merits of the 1.6 and 3.75 micron channels of the AVHRR/3 for cloud detection. Canadian Journal of Remote Sensing, Volume 30, Issue 2, 2004, pp.182-194.

Hunt, G. E., 1973: Radiative properties of terrestrial clouds at visible and infrared thermal window wavelengths. Quart. J. Roy. Meteor. Soc., 99, 346–369.

Inoue, T., 1985: On the temperature and effective emissivity determination of semi-transparent clouds by bi-spectral measurements in the 10 micron window region. J. Meteor. Soc. Japan, 63 (1), 88–89.

Inoue, T., 1987: A cloud type classification with NOAA 7 split window measurements. J. Geophys. Res., 92, 3991-4000.

Joint Polar Satellite System (JPSS) Level 1 Requirements Document (L1RD), Version 1.8, June 25, 2014

Joint Polar Satellite System (JPSS) Program Level 1 Requirements SUPPLEMENT (L1RDS), Version 2.10, June 25, 2014

Joint Polar Satellite System (JPSS) Operational Algorithm Description (OAD) Document for VIIRS Cloud Mask (VCM) Intermediate Product (IP) Software

Joint Polar Satellite System (JPSS) VIIRS Cloud Mask (VCM) Algorithm Theoretical Basis Document (ATBD)

Joro S., Samain O.,Yildirim A., van de Berg L., Lutz H.J.: Towards an improved active fire monitoring product for MSG satellites. 2008.
http://www.eumetsat.int/Home/Main/AboutEUMETSAT/Publications/ConferenceandWorkshopProceedings/2008/SP_1232700911980

Kopp, Thomas J.; Thomas, W.; Heidinger, Andrew K.; Botambekov, Denis; Frey, Richard A.; Hutchison, Keith D.; Iisager, Barbara D.; Brueske, Kurt; and Reed, Bonnie; The VIIRS Cloud Mask: Progress in the first year of S-NPP toward a common cloud detection scheme. Journal of Geophysical Research - Special Issue of the Suomi National Polar-Orbiting Partnership Satellite Calibration, Validation and

Applications, Volume 118, 2013, pp. SNPP403 - SNPP418, doi:10.1002/2013JD020458.

Krebs, W., Mannstein, H., Bugliaro, L., and Mayer, B.: Technical note: A new day- and night-time Meteosat Second Generation Cirrus Detection Algorithm MeCiDA, Atmos. Chem. Phys., 7, 6145-6159, doi:10.5194/acp-7-6145-2007, 2007.

Li, J. and K. Shibata, 2006: On the Effective Solar Pathlength. Journal of the Atmospheric Sciences 2006 63:4, 1365-1373

Moody, E.G., M.D. King, C.B. Schaaf, and S. Platnick, 2008: MODIS-Derived Spatially Complete Surface Albedo Products: Spatial and Temporal Pixel Distribution and Zonal Averages. J. Appl. Meteor. Climatol., 47, 2879–2894.

Pavolonis, M. J., 2009: Advances in extracting cloud composition information from spaceborne infrared radiances: A robust alternative to brightness temperatures. Part II: Proof of concept. Submitted to *J. Atmos. Sci.*

Prabhakara, C., R. S. Fraser, G. Dalu, M. C. Wu, and R. J. Curran, 1988: Thin cirrus clouds: Seasonal distribution over oceans deduced from Nimbus-4 IRIS. J. Appl. Meteor., 27, 379–399.

Schreiner, Anthony J.; Ackerman, Steven A.; Baum, Bryan A. and Heidinger, Andrew K.: A multispectral technique for detecting low-level cloudiness near sunrise. Journal of Atmospheric and Oceanic Technology, Volume 24, Issue 10, 2007, pp.1800-1810.

Seemann, S.W., E. E. Borbas, R. O. Knuteson, G. R. Stephenson, H.-L. Huang, 2007: Development of a Global Infrared Land Surface Emissivity Database for Application to Clear Sky Sounding Retrievals from Multi-spectral Satellite Radiance Measurements. Journal of Applied Meteorology and Climatology, accepted April 2007.

Stowe, L.L., P.A. Davis, and E.P. McClain, 1999: Scientific Basis and Initial Evaluation of the CLAVR-1 Global Clear/Cloud Classification Algorithm for the Advanced Very High Resolution Radiometer. J. Atmos. Oceanic Technol., 16, 656–681.

Thomas, Sarah M.; Heidinger, Andrew K. and Pavolonis, Michael J.: Comparison of NOAA's operational AVHRR-derived cloud amount to other satellite-derived cloud climatologies. Journal of Climate, Volume 17, Issue 24, 2004, pp.4805-4822.

Vaughan, M. A., Winker, D. M., and Powell, K. A.: CALIOP algorithm theoretical basis document. Part 2: Feature detection and layer properties algorithm, PC-SCI-202, Release 1.01, 87 pp., http://www-calipso.larc.nasa.gov/resources/project documentation.php, 2005.

Wang, M., & King, M. D. (1997). Correction of Rayleigh scattering effects in cloud optical thickness retrievals. *Journal of Geophysical Research-Atmospheres*, 102(D22), 25915-25926

Warren, S., 1982. Optical properties of snow, Reviews of Geophysics and Space Physics, 20, 67.

Wu, Xiangqian, W. Paul Menzel, and Gary S. Wade, 1999: Estimation of Sea Surface Temperatures Using GOES-8/9Radiance Measurements. Bulletin of the American Meteorological Society Volume 80, Issue 6 (June 1999) pp. 1127–1138